Available online at www.sciencedirect.com
ScienceDirect
Journal of Computational Physics 225 (2007) 206–236
JOURNAL OF COMPUTATIONAL PHYSICS
www.elsevier.com/locate/jcp

A scalar potential formulation and translation theory for the time-harmonic Maxwell equations

Nail A. Gumerov *,[1], Ramani Duraiswami

Perceptual Interfaces and Reality Laboratory, Institute for Advanced Computer Studies, University of Maryland, College Park, MD 20742, United States

Received 14 February 2006; received in revised form 23 October 2006; accepted 27 November 2006
Available online 16 January 2007

Abstract

We develop a computational method based on the Debye scalar potential representation, which efficiently reduces the solution of Maxwell's equations to the solution of two scalar Helmholtz equations. One of the key contributions of this paper is a theory for the translation of Maxwell solutions using such a representation, since the scalar potential form is not invariant with respect to translations. The translation theory is developed by introducing "conversion" operators, which enable the representation of the electric and magnetic vector fields via scalar potentials in an arbitrary reference frame. Advantages of this representation include the fact that only two Helmholtz equations need be solved, and moreover, the divergence free constraints are satisfied automatically by construction. Truncation error bounds are also presented. The availability of a translation theory and error bounds for this representation can find application in methods such as the Fast Multipole Method.

For illustration of the use of the representation and translation theory we implemented an algorithm for the simulation of Mie scattering off a system of spherical objects of different sizes and dielectric properties using a variant of the T-matrix method. The resulting system was solved using an iterative method based on GMRES. The results of the computations agree well with previous computational and experimental results.

Keywords: Maxwell equations; Debye potentials; Helmholtz equation; Translation operators; Electromagnetic scattering; Mie scattering; T-matrix method; Fast multipole method

1. Introduction

Perhaps there is no need to stress the necessity for efficient numerical solvers for the Maxwell equations in the frequency domain, as they are fundamental to many problems in theoretical and applied electromagnetics. Decomposition of the solutions of these equations into multipole and related series are basic to multiple scattering theory. Due to the vector structure of these equations, the representations involve often unwieldy expressions including series over the vector spherical harmonics. This leads, first, to rather complicated (long)

* Corresponding author. Tel.: +1 301 405 8210.
E-mail address: gumerov@umiacs.umd.edu (N.A. Gumerov).
[1] Also at Fantalgo, LLC.

0021-9991/$ - see front matter
doi:10.1016/j.jcp.2006.11.025

expressions, which themselves can be a source of error, and, second, to excessively large numbers of unknowns in function representations. However, despite these difficulties, researchers have developed the theory for the translation of such series with vector spherical harmonics and methods to compute the translation coefficients (see, e.g., Refs. [23,8,20,6,27]).

It is well-known that any solution of the free-space Maxwell equations can be expressed via two scalar potentials, which are solutions of the scalar Helmholtz equation (see e.g. [18,14]), which are also known as the Debye potentials (Debye's original paper appeared in 1909 [10]). The translation theory for the Helmholtz equation is relatively well developed both for function representations via multipole-type series and the far field signature function (see e.g. [22,11,14]). However, to apply this translation theory to the scalar potential representation of solutions of the Maxwell equations, several issues must be addressed. The purpose of this paper is to provide such a theory. To demonstrate the theory we apply it to Mie scattering problems and compare results to previous calculations and to experiments. Future applications to the fast-multipole accelerated solution of integral equation formulations are envisaged.

In some sense the method which we develop in this paper is similar to the method of translation of solutions of the biharmonic equation that we developed previously [16], where it was shown that any solution of the biharmonic equation can be expressed as a combination of two solutions of the Laplace equations. However, when the biharmonic solution is expressed in this form, the translations cannot be done independently. Instead the two functions must be translated jointly, which can be handled relatively easily by the introduction of the concept of a sparse "conversion" operator. In fact given a fast-multipole method routine for the Laplace equation, we show there that using the conversion operators, it can be employed as a fast-multipole method routine for the biharmonic and polyharmonic equations.

We follow an approach similar to that paper and introduce a potential representation, and the concept of "conversion" operators for the vector Maxwell equations, and show that given a multipole routine for the scalar Helmholtz equation, a routine for the vector Maxwell equations may be obtained using the conversion operators. Of course these conversion operators are different from those for the biharmonic equation. A major difficulty that is faced with the vector representations, of maintaining the divergence free nature of the solution, is avoided by construction.

The method of scalar potentials can be applied for the solution of different boundary value problems, by using truncated series representations. In this paper, for illustrating the use of the scalar potentials and the conversion operators, we demonstrate how they may be used for the solution of multiple scattering problems, such as multiple scattering off many spheres [4,20,28] using a variant of the T-matrix method [21,24,26] with solution of the linear system using a GMRES-based iterative solver. We also provide error bounds that allow selection of the truncation number of the series. The results of the computations satisfy the Maxwell equations by construction, and are validated by an a posteriori check of the error in satisfying the imposed boundary conditions. They are also validated by comparisons with the computational and experimental data of Xu and Gustafson [29,30].

2. Mathematical preliminaries

2.1. The Maxwell equations

In the frequency domain, the phasors of the electric and magnetic field vectors $\mathbf{E}$ and $\mathbf{H}$ for a monochromatic wave of frequency ω satisfy the Maxwell equations

$$\nabla \times \mathbf{E} = \mathrm{i}\omega\mu\mathbf{H}, \quad \nabla \times \mathbf{H} = -\mathrm{i}\omega\epsilon\mathbf{E}, \quad \nabla \cdot \mathbf{E} = 0, \quad \nabla \cdot \mathbf{H} = 0, \tag{1}$$

which in the absence of sources and currents are valid in the carrier medium of electric permittivity ϵ and magnetic permeability μ. As written, these vector equations incorporate eight relations (the equations for the three components of the electric and magnetic fields, and the divergence free constraints).

The solution of these equations is composed of two fields describing incoming and outgoing waves. The latter (radiating) waves satisfy the Silver–Müller radiation conditions

$$\lim_{r\to 0}(\mu^{1/2}\mathbf{H}^{(\mathrm{rad})} \times \mathbf{r} - r\epsilon^{1/2}\mathbf{E}^{(\mathrm{rad})}) = \mathbf{0}, \quad \lim_{r\to 0}(\epsilon^{1/2}\mathbf{E}^{(\mathrm{rad})} \times \mathbf{r} + r\mu^{1/2}\mathbf{H}^{(\mathrm{rad})}) = \mathbf{0}; \quad r = |\mathbf{r}|, \ \mathbf{r} \in \mathbb{R}^3. \tag{2}$$

Let the radiating field have all its singularities inside a sphere of radius a, while the incoming waves are regular by definition everywhere in $\mathbb{R}^3$.

Taking the curl of the first Eq. (1), one can see that in a domain free of singularities the electric field vector, $\mathbf{E}$, satisfies the constrained vector Helmholtz equation

$$(\nabla^2 + k^2)\mathbf{E} = \mathbf{0}, \quad \nabla \cdot \mathbf{E} = 0, \quad k = \omega/c, \tag{3}$$

where k is the wavenumber, c is the speed of light, $c = (\epsilon\mu)^{-1/2}$. The same equations hold for the magnetic field vector, $\mathbf{H}$,

$$(\nabla^2 + k^2)\mathbf{H} = \mathbf{0}, \quad \nabla \cdot \mathbf{H} = 0. \tag{4}$$

It is not difficult to show (e.g., see [14]) that in any given reference frame the electric and magnetic field vectors can be expressed via two scalar potentials, $\phi(\mathbf{r})$ and $\psi(\mathbf{r})$, that characterize the TE and TM partial wave polarization, respectively:

$$\mathbf{E} = \nabla\phi \times \mathbf{r} + \nabla \times (\nabla\psi \times \mathbf{r}), \quad \mathbf{H} = \frac{1}{\mathrm{i}\omega\mu}(k^2\nabla\psi \times \mathbf{r} + \nabla \times (\nabla\phi \times \mathbf{r})), \tag{5}$$

where each potential satisfies the scalar Helmholtz equation

$$(\nabla^2 + k^2)\phi = 0, \quad (\nabla^2 + k^2)\psi = 0. \tag{6}$$

The decomposition of the electric field (5) is equivalent to Eqs. (3) and (4), and therefore, the two scalar functions ϕ and ψ completely characterize the electromagnetic field, and all mathematics related to solution of the Maxwell equations can be expressed in terms of these potentials. We call this method as the "method of scalar potentials" or "method of Debye potentials" [10]. In this theory we work only with ϕ and ψ and the actual values of $\mathbf{E}$ and $\mathbf{H}$ are obtained as needed via direct application of Eq. (5) or by use of some equivalent operators acting on the representations in terms of the scalar functions ϕ and ψ.

2.2. Expansions of solutions over the basis of spherical wave functions

Solutions of the scalar Helmholtz equation can be also decomposed into the incoming and outgoing wave functions. The latter satisfy the Sommerfeld radiation condition

$$\lim_{r\to\infty}\left[r\left(\frac{\partial\phi^{(\mathrm{rad})}}{\partial r} - \mathrm{i}k\phi^{(\mathrm{rad})}\right)\right] = 0, \quad \lim_{r\to\infty}\left[r\left(\frac{\partial\psi^{(\mathrm{rad})}}{\partial r} - \mathrm{i}k\psi^{(\mathrm{rad})}\right)\right] = 0, \tag{7}$$

which are equivalent to the Silver–Müller conditions (2) (e.g. see [14]). Consider a sphere of radius a and a reference frame with origin at the center of this sphere. Solutions singular (radiating) and regular inside the sphere can be expanded as series over the spherical basis functions $S_n^m(\mathbf{r})$ and $R_n^m(\mathbf{r})$, as

$$\phi(\mathbf{r}) = \sum_{n=0}^{\infty}\sum_{m=-n}^{n}\phi_n^m S_n^m(\mathbf{r}) \quad \text{or} \quad \phi(\mathbf{r}) = \sum_{n=0}^{\infty}\sum_{m=-n}^{n}\phi_n^m R_n^m(\mathbf{r}) \tag{8}$$

and similarly for $\psi(\mathbf{r})$. Here

$$R_n^m(\mathbf{r}) = j_n(kr)Y_n^m(\theta,\varphi), \quad S_n^m(\mathbf{r}) = h_n(kr)Y_n^m(\theta,\varphi), \quad n = 0,1,2,\ldots, \quad m = -n,\ldots,n, \tag{9}$$

where $j_n(kr)$ and $h_n(kr)$ are the spherical Bessel and Hankel functions (of the first kind), and $Y_n^m(\theta,\varphi)$ are the orthonormal spherical harmonics:

$$\begin{aligned} Y_n^m(\theta,\varphi) &= (-1)^m\sqrt{\frac{2n+1}{4\pi}\frac{(n-|m|)!}{(n+|m|)!}}P_n^{|m|}(\cos\theta)\mathrm{e}^{\mathrm{i}m\varphi}, \\ P_n^{|m|}(\mu) &= \frac{(-1)^{|m|}}{2^n n!}(1-\mu^2)^{|m|/2}\frac{\mathrm{d}^{|m|+n}}{\mathrm{d}\mu^{|m|+n}}(\mu^2-1)^n, \\ n &= 0,1,2,\ldots; \quad m = -n,\ldots,n, \end{aligned} \tag{10}$$

where $P_n^{|m|}$ are the associated Legendre function expressed above via the Rodrigues formula. Here and below we will use Cartesian (x, y, z) and spherical coordinates (r, θ, φ) related by

$$\mathbf{r} = (x, y, z) = r(\sin\theta\cos\varphi, \sin\theta\sin\varphi, \cos\theta). \tag{11}$$

The traditional way to represent the vectors $\mathbf{E}$ and $\mathbf{H}$ is to insert expansions of type (8) directly into Eq. (5) and obtain, e.g. for the radiating solution:

$$\begin{aligned} &\mathbf{E}(\mathbf{r}) = \sum_{n=0}^{\infty}\sum_{m=-n}^{n}[\phi_n^m \mathbf{M}_n^{(s)m}(\mathbf{r}) + \psi_n^m \mathbf{N}_n^{(s)m}(\mathbf{r})], \\ &\mathbf{M}_n^{(s)m}(\mathbf{r}) = \nabla S_n^m(\mathbf{r}) \times \mathbf{r}, \quad \mathbf{N}_n^{(s)m}(\mathbf{r}) = \nabla \times \mathbf{M}_n^{(s)m}(\mathbf{r}), \end{aligned} \tag{12}$$

where $\mathbf{M}_n^{(s)m}(\mathbf{r})$ and $\mathbf{N}_n^{(s)m}(\mathbf{r})$ are singular spherical vector basis functions, and the ϕ_n^m and ψ_n^m are coefficients of the basis functions (not to be confused with the scalar potential functions ϕ and ψ). This requires heavy use of vector algebra and the translation theory for vector functions. While such theories and methods are available [8,6,27] one of the purposes of the method of scalar potentials is to reduce the complexity by avoiding operations with vector basis functions.

The expansions (8) specify mappings $\{\phi(\mathbf{r}), \psi(\mathbf{r})\} \rightleftarrows \{\mathbf{\Phi}, \mathbf{\Psi}\}$, where $\mathbf{\Phi} = \{\phi_n^m\}$, $\mathbf{\Psi} = \{\psi_n^m\}$ can be thought as matrices, or, more properly, vectors (with a proper alignment of the coefficients) and can be called as function representations in the space of expansion coefficients. When these representations are available in some domain, the functions ϕ and ψ, and so $\mathbf{E}$ and $\mathbf{H}$ can be computed.

2.3. Expressions for operators as matrices relating expansion coefficients

Let $\mathscr{A}$ be a linear operator acting on functions, so that $\widehat{\phi} = \mathscr{A}[\phi]$. Further, let the functions $\widehat{\phi}$ and ϕ be expressed in series over functional bases (which can be the same or different), as in Eq. (9). In this case the operator $\mathscr{A}$ can be represented as a matrix, $\mathbf{A}$, acting on the coefficients of the expansion of ϕ in its basis and transforming them in to the expansion coefficients of $\widehat{\phi}$ in its basis. Thus, the action of the operator on the functions can be written in the equivalent forms

$$\widehat{\phi} = \mathscr{A}[\phi] \rightleftarrows \widehat{\mathbf{\Phi}} = \mathbf{A}\mathbf{\Phi}. \tag{13}$$

The entries of the matrix $\mathbf{A}$ as well as the vectors $\widehat{\mathbf{\Phi}}$ and $\mathbf{\Phi}$ will, in general, depend on the particular expansion bases, and we should indicate this explicitly or implicitly. Since the entries of the vectors $\mathbf{\Phi} = \{\phi_{n'}^{m'}\}$ and $\widehat{\mathbf{\Phi}} = \{\widehat{\phi}_n^m\}$ are each characterized by two indices, the entries of the matrix $\mathbf{A}$ relating them can be characterized by four indices, $A_{nn'}^{mm'} = (\mathbf{A})_{nn'}^{mm'}$.

2.3.1. Differential operators

The first type of linear operators that are important for our development are differential operators. When we differentiate functions, we usually expand the original function and its derivative over the same basis. A remarkable property of the scalar Helmholtz equation is that the matrices representing the differential operators are the same when expressed in either the basis $\{R_n^m(\mathbf{r})\}$ or the basis $\{S_n^m(\mathbf{r})\}$ [14]. The basic first-order differential operators here are

$$\begin{aligned} &\mathscr{D}_z = \frac{1}{k}\frac{\partial}{\partial z}, \quad \mathscr{D}_{x\pm \mathrm{i}y} = \frac{1}{k}\left(\frac{\partial}{\partial x} \pm \mathrm{i}\frac{\partial}{\partial y}\right), \\ &\mathscr{D}_{\mathbf{t}} = \frac{1}{k}\mathbf{t}\cdot\nabla = (t_x + \mathrm{i}t_y)\mathscr{D}_{x-\mathrm{i}y} + (t_x - \mathrm{i}t_y)\mathscr{D}_{x+\mathrm{i}y} + t_z\mathscr{D}_z, \end{aligned} \tag{14}$$

where $\mathbf{t} = (t_x, t_y, t_z)$ is some constant vector. These operators can be represented in the space of coefficients by matrices $\mathbf{D}_z, \mathbf{D}_{x\pm\mathrm{i}y}$, and $\mathbf{D}_{\mathbf{t}}$, respectively. We remark that the matrices corresponding to these operators are very sparse, and may be written as [14]

$$\begin{aligned} (\mathbf{D}_z)_{nn'}^{mm'} &= \delta_{mm'}(a_n^m\delta_{n',n+1} - a_{n'}^m\delta_{n'+1,n}), \\ (\mathbf{D}_{x+\mathrm{i}y})_{nn'}^{mm'} &= \delta_{m',m-1}(b_n^{-m}\delta_{n',n-1} - b_{n'}^{m-1}\delta_{n',n+1}), \\ (\mathbf{D}_{x-\mathrm{i}y})_{nn'}^{mm'} &= \delta_{m',m+1}(b_n^{m}\delta_{n',n-1} - b_{n'}^{-m-1}\delta_{n',n+1}), \end{aligned} \tag{15}$$

where $\delta_{mm'}$ is the Kronecker symbol, and a_n^m and b_n^m are real coefficients defined as

$$a_n^m = a_n^{-m} = \sqrt{\frac{(n+1+m)(n+1-m)}{(2n+1)(2n+3)}}, \quad \text{for } n \geqslant |m|,\ a_n^m = 0,\ \text{for } n < |m|, \tag{16}$$

$$b_n^m = \sqrt{\frac{(n-m-1)(n-m)}{(2n-1)(2n+1)}} \quad \text{for } 0 \leqslant m \leqslant n, \tag{17}$$

$$b_n^m = -\sqrt{\frac{(n-m-1)(n-m)}{(2n-1)(2n+1)}} \quad \text{for } -n \leqslant m < 0,$$

$$b_n^m = 0 \quad \text{for } |m| > n.$$

Instead of using sparse matrices to represent operators, it is sometimes simpler to represent their action via simple relations between the function coefficients. For example, the action of operator $\mathbf{D_t}$ can be written as

$$\begin{aligned}\widehat{\phi}_n^m &= \sum_{n'=0}^{\infty} \sum_{m'=-n'}^{n'} (\mathbf{D_t})_{nn'}^{mm'} \phi_{n'}^{m'} \\ &= (t_x + \mathrm{i}t_y)(b_n^m \phi_{n-1}^{m+1} - b_{n+1}^{-m-1} \phi_{n+1}^{m+1}) + (t_x - \mathrm{i}t_y)(b_n^{-m} \phi_{n-1}^{m-1} - b_{n+1}^{m-1} \phi_{n+1}^{m-1}) + t_z (a_n^m \phi_{n+1}^m - a_{n-1}^m \phi_{n-1}^m).\end{aligned} \tag{18}$$

2.3.2. Translation operators

The second type of linear operator that we wish to express explicitly are the translation operators. In the functional space the translation operator generated by a constant translation vector $\mathbf{t}$ is defined as

$$\widehat{\phi} = \mathscr{T}(\mathbf{t})[\phi], \quad \widehat{\phi}(\mathbf{r}) = \phi(\mathbf{r} + \mathbf{t}). \tag{19}$$

When both ϕ and $\widehat{\phi}$ are represented in basis $\{S_n^m(\mathbf{r})\}$ the matrices representing the multipole-to-multipole translation operator can be denoted as $(\mathbf{S}|\mathbf{S})(\mathbf{t})$. The multipole-to-local operator can be written as $(\mathbf{S}|\mathbf{R})(\mathbf{t})$ (ϕ is in $\{S_n^m(\mathbf{r})\}$ and $\widehat{\phi}$ is in $\{R_n^m(\mathbf{r})\}$), and the local-to-local translation operator as $(\mathbf{R}|\mathbf{R})(\mathbf{t})$ (both ϕ and $\widehat{\phi}$ are in basis $\{R_n^m(\mathbf{r})\}$. We further remark that the entries of the matrices $(\mathbf{S}|\mathbf{S})(\mathbf{t})$ and $(\mathbf{R}|\mathbf{R})(\mathbf{t})$ for the Helmholtz equation are the same for the same translation vector $\mathbf{t}$ [14]. Further, for the Helmholtz equation all matrices for arbitrary $\mathbf{t}$ commute which each other (except for $\mathbf{t} = \mathbf{0}$, which is a singular point for the multipole to regular translation operator $(\mathbf{S}|\mathbf{R})(\mathbf{t})$), and also commute with the matrices representing the differential operators. This observation is the basis for a fast translation method, based on sparse matrix decomposition of the dense translation matrix, and which was first introduced in [14].

Another fast translation method is based on decomposition of the translation vector into a pair of rotations interspersed with translation along the polar axis direction. If needed all entries of the translation matrices can be computed using fast recursive procedures [5,13], which are much faster than direct expression of the matrix coefficients via the 3-j Wigner or similar symbols.

We call the translation operators for the case when the translation direction coincides with the polar z axis, $\mathbf{t} = t\mathbf{i}_z = (0, 0, t)$, as coaxial translation operators. The representation of these operators is more compact, since for coaxial translations the order of the spherical basis functions, m, does not change. In other words, the entries of the coaxial translation matrices have a factor $\delta_{mm'}$, as for the matrix $\mathbf{D}_z$ (see Eq. (15)), which in fact is the coaxial differentiation matrix, since in this case $\mathbf{D_t} = \mathbf{D}_z$. So performing a matrix–vector product with the coaxial translation matrix requires fewer operations than the general translation and can be used in decompositions of the general translation matrix [20]. The coaxial translation operators also can be computed by a faster recursive procedures than those needed in the general case [13].

2.3.3. Rotation Operators

The third type of operators, which we mention are the rotation operators, defined as

$$\widehat{\phi} = \mathscr{R}ot(\mathbf{Q})[\phi], \quad \widehat{\phi}(\widehat{\mathbf{r}}) = \phi(\mathbf{r}), \quad \widehat{\mathbf{r}} = \mathbf{Q}\mathbf{r}, \tag{20}$$

where $\mathbf{r}$ and $\hat{\mathbf{r}}$ are coordinates of the radius-vector in the original and rotated reference frame, assuming that the rotation transform in three dimensions is performed with real 3×3 rotation matrix $\mathbf{Q}$. The rotation operator can also be represented by a matrix, $\mathbf{Rot}(\mathbf{Q})$. The entries of this matrix are proportional to $\delta_{nn'}$. In other words, the rotation transform does not change the degree of the spherical basis functions. This makes the rotation operator more compact than general translation operator, and this can be used in decompositions of the translation matrix. Also the entries of matrix $\mathbf{Rot}(\mathbf{Q})$ can be computed by fast recursive procedures [13,14].

As mentioned before, a particularly important type of decomposition of a translation operator is the rotation-coaxial translation decomposition, where we decompose the general translation operation into a rotation of the reference frame to align the z axis with the direction of translation vector $\mathbf{t}$, then translate along the z axis ("coaxial translation"), and then rotate back to obtain the original axes orientation.

If p is the truncation number at which we truncate all expansions with $n = 0, \ldots, p-1, m = -n, \ldots, n$ (so we hold only p^2 terms in each of the expansions (8)), the general translation matrix has p^4 entries, and a computation of a general translation via a matrix–vector product requires $O(p^4)$ operations, while the rotation-coaxial translation decomposition requires $O(p^3)$ operations.

3. Method of scalar potentials

3.1. Translations of vector functions

We must extend the translation operators for scalar Helmholtz functions introduced above to the case of the vector Maxwell functions. Since

$$\begin{aligned} &\widehat{\mathbf{E}}(\mathbf{r}) = \mathbf{E}(\mathbf{r}+\mathbf{t}) = \nabla \times (\mathbf{r}\widehat{\phi}) + \nabla \times \nabla \times (\mathbf{r}\widehat{\psi}) + \nabla \times (\mathbf{t}\widehat{\phi}) + \nabla \times \nabla \times (\mathbf{t}\widehat{\psi}), \\ &\widehat{\mathbf{E}} = \mathscr{T}(\mathbf{t})[\mathbf{E}], \quad \widehat{\phi} = \mathscr{T}(\mathbf{t})[\phi], \quad \widehat{\psi} = \mathscr{T}(\mathbf{t})[\psi], \end{aligned} \tag{21}$$

we see that the translated function is not represented in the same form as the original function in terms of the Debye potentials. At first glance, representing the translations via scalar potentials (5), thus seems a non-trivial task. In fact, to retain the scalar potential form for $\widehat{\mathbf{E}}(\mathbf{r})$ in a basis centered at $\mathbf{r} = \mathbf{0}$ we must express it in the form

$$\widehat{\mathbf{E}}(\mathbf{r}) = \nabla \times (\mathbf{r}\tilde{\phi}) + \nabla \times \nabla \times (\mathbf{r}\tilde{\psi}), \tag{22}$$

for some other potentials $\tilde{\phi}$ and $\tilde{\psi}$. Due to linearity of all operations the functions $\tilde{\phi}$ and $\tilde{\psi}$ should linearly depend on $\widehat{\phi}$ and $\widehat{\psi}$. Such a linear dependence is provided by conversion operators, which are defined then as

$$\begin{aligned} \tilde{\phi} &= \mathscr{C}_{11}[\widehat{\phi}] + \mathscr{C}_{12}[\widehat{\psi}], \\ \tilde{\psi} &= \mathscr{C}_{21}[\widehat{\phi}] + \mathscr{C}_{22}[\widehat{\psi}]. \end{aligned} \tag{23}$$

The conversion operators can be represented as matrices acting on coefficients over the spherical wave function basis. It is natural to represent $(\tilde{\phi}, \tilde{\psi})$ in the same basis as $(\widehat{\phi}, \widehat{\psi})$, and in this case it is not difficult to see that the entries of the conversion operators will not depend on which basis $\{S_n^m(\mathbf{r})\}$ or $\{R_n^m(\mathbf{r})\}$ we use. Indeed, as mentioned above the differential operators for scalar functions are the same for the both bases, while the conversion operators can be expressed in terms of such operators. So Eq. (23) imply

$$\begin{aligned} \widetilde{\mathbf{\Phi}} &= \mathbf{C}_{11}\widehat{\mathbf{\Phi}} + \mathbf{C}_{12}\widehat{\mathbf{\Psi}}, \\ \widetilde{\mathbf{\Psi}} &= \mathbf{C}_{21}\widehat{\mathbf{\Phi}} + \mathbf{C}_{22}\widehat{\mathbf{\Psi}}. \end{aligned} \tag{24}$$

Note that due to the symmetry in representation of the electric and magnetic field vectors (5) (the replacement of ϕ with $(\mathrm{i}\omega\mu)^{-1}k^2\psi$ and ψ with $(\mathrm{i}\omega\mu)^{-1}\phi$ results in the same conversion operation. For the magnetic field vector, we have

$$\mathbf{C}_{11} = \mathbf{C}_{22}, \quad \mathbf{C}_{12} = k^2\mathbf{C}_{21}. \tag{25}$$

Below we derive explicit expressions for these matrices. We show that these matrices are sparse and the computational cost of the conversion procedure is low in terms of memory and time.

3.2. Conversion operators

Let us represent the functions $\tilde{\phi}$ and $\tilde{\psi}$ in the form

$$\tilde{\phi} = \widehat{\phi} + \phi', \quad \tilde{\psi} = \widehat{\psi} + \psi'. \tag{26}$$

As follows from Eqs. (21) and (22) the functions marked with primes satisfy

$$\nabla \times (\mathbf{r}\phi') + \nabla \times \nabla \times (\mathbf{r}\psi') = \nabla \times (\mathbf{t}\widehat{\phi}) + \nabla \times \nabla \times (\mathbf{t}\widehat{\psi}). \tag{27}$$

The scalar product of both sides of this equation with the vector $\mathbf{r}$ yields

$$\mathbf{r} \cdot \nabla \times \nabla \times (\mathbf{r}\psi') = \mathbf{r} \cdot \nabla \times (\mathbf{t}\widehat{\phi}) + \mathbf{r} \cdot \nabla \times \nabla \times (\mathbf{t}\widehat{\psi}), \tag{28}$$

due to the relations

$$\nabla \times \nabla \times (\mathbf{r}\psi') = \nabla(\psi' + \mathbf{r} \cdot \nabla\psi') + k^2\mathbf{r}\psi', \tag{29}$$

$$\nabla \times \nabla \times (\mathbf{t}\widehat{\psi}) = \nabla(\mathbf{t} \cdot \nabla\widehat{\psi}) + k^2\mathbf{t}\widehat{\psi}, \tag{30}$$

$$\mathbf{r} \cdot \nabla \times (\mathbf{t}\widehat{\phi}) = -(\mathbf{r} \times \mathbf{t}) \cdot \nabla\widehat{\phi}. \tag{31}$$

To prove relation (29), we note that

$$\nabla^2(x\psi') = x\nabla^2\psi' + 2\nabla x \cdot \nabla\psi' + \psi'\nabla^2 x = x\nabla^2\psi' + 2\frac{\partial\psi'}{\partial x}. \tag{32}$$

A similar expression holds if we replace the coordinate x with y or z. Therefore, for vector $\mathbf{r} = \mathbf{i}_x x + \mathbf{i}_y y + \mathbf{i}_z z$ we have

$$\nabla^2(\mathbf{r}\psi') = \mathbf{r}\nabla^2\psi' + 2\nabla\psi'. \tag{33}$$

Now using the well-known expression for the Laplacian of the vector function via the curl of curl and gradient of divergence and the fact that ψ' satisfies the scalar Helmholtz equation, we obtain

$$\begin{aligned}\nabla \times \nabla \times (\mathbf{r}\psi') &= \nabla[\nabla \cdot (\mathbf{r}\psi')] - \nabla^2(\mathbf{r}\psi') = \nabla(\psi'\nabla \cdot \mathbf{r} + \mathbf{r} \cdot \nabla\psi') - \mathbf{r}\nabla^2\psi' - 2\nabla\psi' \\ &= \nabla(3\psi' + \mathbf{r} \cdot \nabla\psi' - 2\psi') + k^2\mathbf{r}\psi' = \nabla(\psi' + \mathbf{r} \cdot \nabla\psi') + k^2\mathbf{r}\psi'.\end{aligned} \tag{34}$$

Introducing the following differential operators

$$\begin{aligned}&\mathscr{D}_{rr} = r^2\frac{\partial^2}{\partial r^2} + 2r\frac{\partial}{\partial r} + k^2r^2, \quad \mathscr{D}_{\mathbf{r}\times\mathbf{t}} = (\mathbf{r} \times \mathbf{t}) \cdot \nabla, \\ &\mathscr{D}_{\mathbf{r}\cdot\mathbf{t}} = (\mathbf{r} \cdot \nabla)(\mathbf{t} \cdot \nabla) + k^2(\mathbf{r} \cdot \mathbf{t}),\end{aligned} \tag{35}$$

we can rewrite Eq. (28) in the form

$$\mathscr{D}_{rr}[\psi'] = -\mathscr{D}_{\mathbf{r}\times\mathbf{t}}[\widehat{\phi}] + \mathscr{D}_{\mathbf{r}\cdot\mathbf{t}}[\widehat{\psi}]. \tag{36}$$

Consider the action of operator $\mathscr{D}_{rr}$ on a spherical basis function (9) (since the singular and regular basis functions satisfy the same recurrence relations, it is sufficient to consider only one of them, say the regular basis functions):

$$\mathscr{D}_{rr}[R_n^m(\mathbf{r})] = Y_n^m(\theta,\varphi)\mathscr{D}_{rr}[j_n(kr)] = Y_n(\theta,\varphi)n(n+1)j_n(kr) = n(n+1)R_n^m(\mathbf{r}). \tag{37}$$

This holds because the spherical Bessel (and Hankel) functions are eigenfunctions of $\mathscr{D}_{rr}$ corresponding to the eigenvalue $n(n+1)$. This means that in the space of expansion coefficients, for expansions of type (8), $\mathscr{D}_{rr}$ is represented by a diagonal matrix $\mathbf{D}_{rr}$, with entries

$$(\mathbf{D}_{rr})_{nn'}^{mm'} = n(n+1)\delta_{mm'}\delta_{nn'}, \quad n,n' = 0,1,\ldots, \quad m = -n,\ldots,n, \quad m' = -n',\ldots,n'. \tag{38}$$

This also shows that the function ψ' is determined up to an arbitrary function of r (indeed $\nabla \times (\mathbf{r}f(r)) = \mathbf{0}$), which in case of spherical basis functions is proportional to the zero-order Bessel function. This function can

be deliberately set to zero, since in any case it does not contribute either to $\mathbf{E}(\mathbf{r})$, or to $\mathbf{H}(\mathbf{r})$. Accepting this convention, we can define the inverse operator $\mathscr{D}_{rr}^{-1}$ as an operator, represented by the diagonal matrix

$$(\mathbf{D}_{rr}^{-1})_{nn'}^{mm'} = \frac{1}{n(n+1)}\delta_{mm'}\delta_{nn'}, \quad n,n' > 0, \quad (\mathbf{D}_{rr}^{-1})_{00}^{00} = 0. \tag{39}$$

The matrix representations of the operators $\mathscr{D}_{\mathbf{r}\times\mathbf{t}}$ and $\mathscr{D}_{\mathbf{r}\cdot\mathbf{t}}$ are more involved and we show how one can derive expressions for their entries in Appendix A. Similar to Eq. (18), it is convenient to write the results of the action of these matrices on the coefficients of some function χ:

$$\widehat{\chi}_n^m = \sum_{n'=0}^{\infty}\sum_{m'=-n'}^{n'}(\mathbf{D}_{\mathbf{r}\times\mathbf{t}})_{nn'}^{mm'}\chi_{n'}^{m'} = \frac{\mathrm{i}}{2}(t_{x+\mathrm{i}y}c_n^m\chi_n^{m+1} + t_{x-\mathrm{i}y}c_n^{m-1}\chi_n^{m-1} - 2mt_z\chi_n^m), \; t_{x\pm\mathrm{i}y} = t_x \pm \mathrm{i}t_y \tag{40}$$

$$\begin{aligned}\widehat{\chi}_n^m &= \sum_{n'=0}^{\infty}\sum_{m'=-n'}^{n'}(\mathbf{D}_{\mathbf{r}\cdot\mathbf{t}})_{nn'}^{mm'}\chi_{n'}^{m'} \\ &= -\frac{k}{2}\{t_{x+\mathrm{i}y}[nb_{n+1}^{-m-1}\chi_{n+1}^{m+1} + (n+1)b_n^m\chi_{n-1}^{m+1}] + t_{x-\mathrm{i}y}[nb_{n+1}^{m-1}\chi_{n+1}^{m-1} + (n+1)b_n^{-m}\chi_{n-1}^{m-1}] \\ &\quad - 2t_z[na_n^m\chi_{n+1}^m + (n+1)a_{n-1}^m\chi_{n-1}^m]\},\end{aligned} \tag{41}$$

where c_n^m are real coefficients describing infinitesimal rotation, defined as

$$c_n^m = \begin{cases} \sqrt{(n-m)(n+m+1)} & \text{for } 0 \leqslant m \leqslant n \\ -\sqrt{(n-m)(n+m+1)} & \text{for } -n \leqslant m < 0 \\ 0 & \text{for } |m| > n \end{cases}. \tag{42}$$

These expressions yield the following expressions, which represent the action of the conversion matrices:

$$\begin{aligned}\tilde{\psi}_n^m &= \widehat{\psi}_n^m - \frac{1}{2n(n+1)}\Big\{\mathrm{i}(t_{x+\mathrm{i}y}c_n^m\widehat{\phi}_n^{m+1} + t_{x-\mathrm{i}y}c_n^{m-1}\widehat{\phi}_n^{m-1} - 2mt_z\widehat{\phi}_n^m) + k\{t_{x+\mathrm{i}y}[nb_{n+1}^{-m-1}\widehat{\psi}_{n+1}^{m+1} + (n+1)b_n^m\widehat{\psi}_{n-1}^{m+1}]\} \\ &\quad + kt_{x-\mathrm{i}y}[nb_{n+1}^{m-1}\widehat{\psi}_{n+1}^{m-1} + (n+1)b_n^{-m}\widehat{\psi}_{n-1}^{m-1}] - 2kt_z[na_n^m\widehat{\psi}_{n+1}^m + (n+1)a_{n-1}^m\widehat{\psi}_{n-1}^m]\Big\}, \\ &\quad n = 1,2,\ldots, \quad m = -n,\ldots,n, \quad t_{x\pm iy} = t_x \pm it_y,\end{aligned} \tag{43}$$

$$\begin{aligned}\tilde{\phi}_n^m &= \widehat{\phi}_n^m - \frac{1}{2n(n+1)}\Big\{\mathrm{i}k^2(t_{x+\mathrm{i}y}c_n^m\widehat{\psi}_n^{m+1} + t_{x-\mathrm{i}y}c_n^{m-1}\widehat{\psi}_n^{m-1} - 2mt_z\widehat{\psi}_n^m) + kt_{x+\mathrm{i}y}[nb_{n+1}^{-m-1}\widehat{\phi}_{n+1}^{m+1} + (n+1)b_n^m\widehat{\phi}_{n-1}^{m+1}] \\ &\quad + kt_{x-\mathrm{i}y}[nb_{n+1}^{m-1}\widehat{\phi}_{n+1}^{m-1} + (n+1)b_n^{-m}\widehat{\phi}_{n-1}^{m-1}] - 2kt_z[na_n^m\widehat{\phi}_{n+1}^m + (n+1)a_{n-1}^m\widehat{\phi}_{n-1}^m]\Big\}, \\ &\quad n = 1,2,\ldots, \quad m = -n,\ldots,n, \quad t_{x\pm\mathrm{i}y} = t_x \pm \mathrm{i}t_y,\end{aligned} \tag{44}$$

where the latter relation between $\tilde{\phi}_n^m$ and $(\widehat{\phi}_n^m, \widehat{\psi}_n^m)$ follows from the symmetry relation (25).

3.3. Rotation-coaxial translation decomposition

We remark that the rotation transform defined by (20) does not change the form of decomposition (5) as **E** and **H** are treated as physical vectors, which are invariant objects with respect to the selection of the reference frame, and **r** and $\widehat{\mathbf{r}}$ are referred to the same point in the physical space. Thus in the rotated reference frame we have for the electric field vector

$$\widehat{\mathbf{E}}(\widehat{\mathbf{r}}) = \nabla\times(\widehat{\mathbf{r}}\widehat{\phi}) + \nabla\times\nabla\times(\widehat{\mathbf{r}}\widehat{\psi}). \tag{45}$$

Furthermore, expressions for the conversion operators (43) and (44) are substantially simpler for coaxial translations, $\mathbf{t} = t\mathbf{i}_z$:

$$\begin{aligned}\tilde{\psi}_n^m &= \widehat{\psi}_n^m + \frac{t}{n(n+1)}\{\mathrm{i}m\widehat{\phi}_n^m + k[na_n^m\widehat{\psi}_{n+1}^m + (n+1)a_{n-1}^m\widehat{\psi}_{n-1}^m]\}, \\ \tilde{\phi}_n^m &= \widehat{\phi}_n^m + \frac{t}{n(n+1)}\{\mathrm{i}k^2m\widehat{\psi}_n^m + k[na_n^m\widehat{\phi}_{n+1}^m + (n+1)a_{n-1}^m\widehat{\phi}_{n-1}^m]\}, \\ &\quad n = 1,2,\ldots, \quad m = -n,\ldots,n.\end{aligned} \tag{46}$$

So the rotation-coaxial translation decompositions again appears to be an efficient computational procedure.

We also note that using the notation (24) and (25) we can see that general translation preserving the scalar potential form (5) can be written as

$$\begin{pmatrix} \widetilde{\mathbf{\Phi}} \\ \widetilde{\mathbf{\Psi}} \end{pmatrix} = \begin{pmatrix} \mathbf{C}_{11}(\mathbf{t}) & k^2\mathbf{C}_{21}(\mathbf{t}) \\ \mathbf{C}_{21}(\mathbf{t}) & \mathbf{C}_{11}(\mathbf{t}) \end{pmatrix} \begin{pmatrix} \mathbf{T}(\mathbf{t}) & \mathbf{0} \\ \mathbf{0} & \mathbf{T}(\mathbf{t}) \end{pmatrix} \begin{pmatrix} \mathbf{\Phi} \\ \mathbf{\Psi} \end{pmatrix}, \tag{47}$$

where $\mathbf{T}(\mathbf{t})$ is the translation matrix for scalar functions (e.g. $(\mathbf{R}|\mathbf{R})(\mathbf{t})$). In the rotation-coaxial translation decomposition this matrix can be represented as

$$\mathbf{T}(\mathbf{t}) = \mathbf{Rot}^{-1}(\mathbf{Q}(\mathbf{t}))\mathbf{T}^{\mathrm{coax}}(t)\mathbf{Rot}(\mathbf{Q}(\mathbf{t})). \tag{48}$$

On the other hand we have

$$\begin{aligned} \begin{pmatrix} \widetilde{\mathbf{\Phi}} \\ \widetilde{\mathbf{\Psi}} \end{pmatrix} = & \begin{pmatrix} \mathbf{Rot}^{-1}(\mathbf{Q}(\mathbf{t})) & \mathbf{0} \\ \mathbf{0} & \mathbf{Rot}^{-1}(\mathbf{Q}(\mathbf{t})) \end{pmatrix} \begin{pmatrix} \mathbf{C}_{11}^{\mathrm{coax}}(t) & k^2\mathbf{C}_{21}^{\mathrm{coax}}(t) \\ \mathbf{C}_{21}^{\mathrm{coax}}(t) & \mathbf{C}_{11}(t) \end{pmatrix} \\ & \times \begin{pmatrix} \mathbf{T}^{\mathrm{coax}}(t) & \mathbf{0} \\ \mathbf{0} & \mathbf{T}^{\mathrm{coax}}(t) \end{pmatrix} \begin{pmatrix} \mathbf{Rot}(\mathbf{Q}(\mathbf{t})) & \mathbf{0} \\ \mathbf{0} & \mathbf{Rot}(\mathbf{Q}(\mathbf{t})) \end{pmatrix} \begin{pmatrix} \mathbf{\Phi} \\ \mathbf{\Psi} \end{pmatrix}. \end{aligned} \tag{49}$$

It is not difficult to directly check, that Eqs. (47)–(49) result in the following relations

$$\mathbf{C}_{11}(\mathbf{t}) = \mathbf{Rot}^{-1}(\mathbf{Q}(\mathbf{t}))\mathbf{C}_{11}^{\mathrm{coax}}(t)\mathbf{Rot}(\mathbf{Q}(\mathbf{t})), \quad \mathbf{C}_{21}(\mathbf{t}) = \mathbf{Rot}^{-1}(\mathbf{Q}(\mathbf{t}))\mathbf{C}_{21}^{\mathrm{coax}}(t)\mathbf{Rot}(\mathbf{Q}(\mathbf{t})), \tag{50}$$

where the action of coaxial conversion operators $\mathbf{C}_{11}^{\mathrm{coax}}(t)$ and $\mathbf{C}_{21}^{\mathrm{coax}}(t)$ follows from Eqs (46). We also can note that the operator $\mathscr{D}_{rr}$ defined by Eq. (35) is invariant with respect to the rotation transform, which preserves the length of the radius-vector. So decompositions (50) can be combined with the form (36) for conversion operation, resulting in

$$\mathbf{D}_{\mathbf{r}\times\mathbf{t}} = t\mathbf{Rot}^{-1}(\mathbf{Q}(\mathbf{t}))\mathbf{D}_{\mathbf{r}\times\mathbf{i}_z}\mathbf{Rot}(\mathbf{Q}(\mathbf{t})), \quad \mathbf{D}_{\mathbf{r}\cdot\mathbf{t}} = t\mathbf{Rot}^{-1}(\mathbf{Q}(\mathbf{t}))\mathbf{D}_{\mathbf{r}\cdot\mathbf{i}_z}\mathbf{Rot}(\mathbf{Q}(\mathbf{t})), \tag{51}$$

where the matrices $\mathbf{D}_{\mathbf{r}\times\mathbf{i}_z}$ and $\mathbf{D}_{\mathbf{r}\cdot\mathbf{i}_z}$ do not depend on t as they represent the operators

$$\mathscr{D}_{\mathbf{r}\times\mathbf{i}_z} = (\mathbf{r}\times\mathbf{i}_z)\cdot\nabla, \quad \mathscr{D}_{\mathbf{r}\cdot\mathbf{i}_z} = (\mathbf{r}\cdot\nabla)(\mathbf{i}_z\cdot\nabla) + k^2(\mathbf{r}\cdot\mathbf{i}_z). \tag{52}$$

3.4. Computation of components of vector fields

One more operation for the method of scalar potentials needs to be specified. Given scalar functions ϕ and ψ we should have an efficient procedure to compute components of electric and magnetic field vectors according Eq. (5). While this can be done directly using Eq. (5), finite differences, and samples of ϕ and ψ, more accurate, fast, and consistent way to do this is to obtain expansion coefficients for the components of these vectors using expansion coefficients of the scalar potentials.

Consider the projection of the electric field vector on some direction $\mathbf{t}$. We have (29), where ψ' can be replaced with ψ, (35), (14), and the fact that $(\mathbf{t}\cdot\nabla)(\mathbf{r}\cdot\nabla) = (\mathbf{r}\cdot\nabla)(\mathbf{t}\cdot\nabla) + \mathbf{t}\cdot\nabla$:

$$\begin{aligned} E_t = \mathbf{t}\cdot\mathbf{E} &= \mathbf{t}\cdot[\nabla\phi\times\mathbf{r} + \nabla\times(\nabla\psi\times\mathbf{r})] = (\mathbf{r}\times\mathbf{t})\cdot\nabla\phi + \mathbf{t}\cdot[\nabla(\psi + \mathbf{r}\cdot\nabla\psi) + k^2\mathbf{r}\psi] \\ &= (\mathbf{r}\times\mathbf{t})\cdot\nabla\phi + 2\mathbf{t}\cdot\nabla\psi + [(\mathbf{r}\cdot\nabla)(\mathbf{t}\cdot\nabla) + k^2(\mathbf{r}\cdot\mathbf{t})]\psi = \mathscr{D}_{\mathbf{r}\times\mathbf{t}}[\phi] + 2k\mathscr{D}_{\mathbf{t}}[\psi] + \mathscr{D}_{\mathbf{r}\cdot\mathbf{t}}[\psi]. \end{aligned} \tag{53}$$

As E_t satisfies the scalar Helmholtz equation, this function can be expanded into the series over the same functional basis as ϕ and ψ. Denoting respective expansion coefficients as $(E_t)_n^m$ and using expressions for representations of operators $\mathscr{D}_{\mathbf{r}\times\mathbf{t}}$, $\mathscr{D}_{\mathbf{t}}$, and $\mathscr{D}_{\mathbf{r}\cdot\mathbf{t}}$, we obtain

$$\begin{aligned} (E_t)_n^m = \frac{1}{2}\big\{ & \mathrm{i}(t_{x+\mathrm{i}y}c_n^m\phi_n^{m+1} + t_{x-\mathrm{i}y}c_n^{m-1}\phi_n^{m-1} - 2mt_z\phi_n^m) - k\big\{t_{x+\mathrm{i}y}[(n+2)b_{n+1}^{-m-1}\psi_{n+1}^{m+1} + (n-1)b_n^m\psi_{n-1}^{m+1}] \\ & + t_{x-\mathrm{i}y}[(n+2)b_{n+1}^{m-1}\psi_{n+1}^{m-1} + (n-1)b_n^{-m}\psi_{n-1}^{m-1}] - 2t_z[(n+2)a_n^m\psi_{n+1}^m + (n-1)a_{n-1}^m\psi_{n-1}^m]\big\}\big\}. \end{aligned} \tag{54}$$

The same type of expression can be written for the projection of the magnetic field vector, $(H_t)_n^m$ by replacing ϕ with $(\mathrm{i}\omega\mu)^{-1}k^2\psi$ and ψ with $(\mathrm{i}\omega\mu)^{-1}\phi$. For convenience of the reader, we list the expansion coefficients for the

Cartesian components of the electric field vector, which follow from Eq. (54) by setting $(t_x, t_y, t_z) = (1,0,0), (0,1,0),$ and $(0,0,1)$, respectively:

$$\begin{aligned}
(E_x)_n^m &= \frac{\mathrm{i}}{2}[c_n^{m-1}\phi_n^{m-1} + c_n^m\phi_n^{m+1}] \\
&\quad - \frac{k}{2}[(n+2)b_{n+1}^{m-1}\psi_{n+1}^{m-1} + (n-1)b_n^{-m}\psi_{n-1}^{m-1} + (n+2)b_{n+1}^{-m-1}\psi_{n+1}^{m+1} + (n-1)b_n^m\psi_{n-1}^{m+1}], \\
(E_y)_n^m &= -\frac{1}{2}[-c_n^{m-1}\phi_n^{m-1} + c_n^m\phi_n^{m+1}] \\
&\quad + \frac{\mathrm{i}k}{2}[(n+2)b_{n+1}^{m-1}\psi_{n+1}^{m-1} + (n-1)b_n^{-m}\psi_{n-1}^{m-1} - (n+2)b_{n+1}^{-m-1}\psi_{n+1}^{m+1} - (n-1)b_n^m\psi_{n-1}^{m+1}], \\
(E_z)_n^m &= -\mathrm{i}m\phi_n^m + k[(n+2)a_n^m\psi_{n+1}^m + (n-1)a_{n-1}^m\psi_{n-1}^m].
\end{aligned} \tag{55}$$

Note also that $\mathbf{E}\cdot\mathbf{r}$ is a scalar function, that satisfies the Helmholtz equation, and according to Eqs. (5), (29), and (35) it is simply related to function ψ:

$$\mathbf{r}\cdot\mathbf{E} = \mathscr{D}_{rr}[\psi], \quad (\mathbf{r}\cdot\mathbf{E})_n^m = n(n+1)\psi_n^m. \tag{56}$$

Similarly,

$$\mathbf{r}\cdot(\nabla\times\mathbf{E}) = \mathscr{D}_{rr}[\phi], \quad [\mathbf{r}\cdot(\nabla\times\mathbf{E})]_n^m = n(n+1)\phi_n^m. \tag{57}$$

The latter two expressions specify operations, which in some sense are inverse to (55). Indeed, while Eq. (55) allow us to get $\mathbf{E}$ from given ϕ and ψ, Eqs. (56) and (57) can be used for determination of ϕ and ψ from given $\mathbf{E}$.

Again as in the case of conversion operators, we can see that physical components of the fields can be computed using rapid procedures, and can be represented via sparse matrices.

4. Representation of elementary solutions

4.1. Plane wave expansions

The method of Debye potentials can be used for solution of different electromagnetic scattering problems. In typical formulations the incident field is taken in the form of a plane wave:

$$\mathbf{E} = (\mathbf{s}\times\mathbf{q})\mathrm{e}^{\mathrm{i}k\mathbf{s}\cdot\mathbf{r}}, \tag{58}$$

where $\mathbf{s}$ is the direction of wave propagation and $\mathbf{q}$ is an arbitrary unit vector. To represent this field in the form (5) we can take the scalar product of the electromagnetic vector and $\mathbf{r}$ to obtain

$$\mathscr{D}_{rr}[\psi] = \mathbf{r}\cdot\mathbf{E} = \mathbf{r}\cdot(\mathbf{s}\times\mathbf{q})\mathrm{e}^{\mathrm{i}k\mathbf{s}\cdot\mathbf{r}} = -(\mathbf{r}\times\mathbf{q})\cdot\mathbf{s}\mathrm{e}^{\mathrm{i}k\mathbf{s}\cdot\mathbf{r}} = -\frac{1}{\mathrm{i}k}(\mathbf{r}\times\mathbf{q})\cdot\nabla\mathrm{e}^{\mathrm{i}k\mathbf{s}\cdot\mathbf{r}}. \tag{59}$$

Consider the Gegenbauer expansion for the plane-wave

$$\mathrm{e}^{\mathrm{i}k\mathbf{s}\cdot\mathbf{r}} = 4\pi\sum_{n=0}^{\infty}\sum_{m=-n}^{n}\mathrm{i}^n Y_n^{-m}(\mathbf{s})R_n^m(\mathbf{r}). \tag{60}$$

Thus we have

$$-\frac{1}{\mathrm{i}k}(\mathbf{r}\times\mathbf{q})\cdot\nabla\mathrm{e}^{\mathrm{i}k\mathbf{s}\cdot\mathbf{r}} = \sum_{n=0}^{\infty}\sum_{m=-n}^{n}A_n^m R_n^m(\mathbf{r}), \tag{61}$$

where

$$A_n^m = -\frac{4\pi\mathrm{i}^n}{k}\left\{\frac{1}{2}[(q_x+\mathrm{i}q_y)c_n^m Y_n^{-m-1}(\mathbf{s}) + (q_x-\mathrm{i}q_y)c_n^{m-1}Y_n^{-m+1}(\mathbf{s})] - mq_z Y_n^{-m}(\mathbf{s})\right\}. \tag{62}$$

Using the inversion of the operator $\mathscr{D}_{rr}$ in the space of expansion coefficients (39), we obtain

$$\psi_n^m = -\frac{4\pi \mathrm{i}^n}{n(n+1)k}\left\{\frac{1}{2}[(q_x + \mathrm{i}q_y)c_n^m Y_n^{-m-1}(\mathbf{s}) + (q_x - \mathrm{i}q_y)c_n^{m-1} Y_n^{-m+1}(\mathbf{s})] - mq_z Y_n^{-m}(\mathbf{s})\right\}, \quad n = 1, 2, \ldots, \quad m = -n, \ldots, n. \tag{63}$$

To determine the function ϕ we take the curl of the electric field vector:

$$\nabla \times \mathbf{E} = \nabla \times [(\mathbf{s} \times \mathbf{q})\mathrm{e}^{\mathrm{i}k\mathbf{s}\cdot\mathbf{r}}] = \mathrm{i}k(\mathbf{s} \times \mathbf{p})\mathrm{e}^{\mathrm{i}k\mathbf{s}\cdot\mathbf{r}}, \quad \mathbf{p} = \mathbf{s} \times \mathbf{q}. \tag{64}$$

We have then:

$$\mathscr{D}_{rr}[\phi] = \mathbf{r} \cdot (\nabla \times \mathbf{E}) = \mathrm{i}k\mathbf{r} \cdot [\mathbf{s} \times (\mathbf{s} \times \mathbf{q})]\mathrm{e}^{\mathrm{i}k\mathbf{s}\cdot\mathbf{r}} = -\mathrm{i}k[\mathbf{r} \times (\mathbf{s} \times \mathbf{q})] \cdot \mathbf{s}\mathrm{e}^{\mathrm{i}k\mathbf{s}\cdot\mathbf{r}} = -[\mathbf{r} \times (\mathbf{s} \times \mathbf{q})] \cdot \nabla \mathrm{e}^{\mathrm{i}k\mathbf{s}\cdot\mathbf{r}}. \tag{65}$$

We obtain then similar to the previous result coefficients for function ϕ:

$$\phi_n^m = -\frac{4\pi \mathrm{i}^{n+1}}{n(n+1)}\left\{\frac{1}{2}[(p_x + \mathrm{i}p_y)c_n^m Y_n^{-m-1}(\mathbf{s}) + (p_x - \mathrm{i}p_y)c_n^{m-1} Y_n^{-m+1}(\mathbf{s})] - mp_z Y_n^{-m}(\mathbf{s})\right\}, \quad n = 1, 2, \ldots, \quad m = -n, \ldots, n. \tag{66}$$

4.2. Electric and magnetic dipoles

Another elementary solution of the Maxwell equations in a homogeneous medium is produced by a point singularity (point current source). This field, known as the field of Hertzian dipole of moment $\mathbf{p}$, produces the electric field vector

$$\mathbf{E}(\mathbf{r}) = \left(\mathbf{I} + \frac{\nabla\nabla}{k^2}\right) \cdot [\mathbf{p}G(\mathbf{r})] = \mathbf{p}G + \frac{1}{k^2}\nabla(\mathbf{p} \cdot \nabla G), \tag{67}$$

where $\mathbf{I}$ and $\nabla\nabla$ are the unity and differentiation dyadic tensors, and $G(\mathbf{r})$ is the free-space Green's function for scalar Helmholtz equation, for a source centered at the origin of the reference frame:

$$G(\mathbf{r}) = \frac{\mathrm{e}^{\mathrm{i}kr}}{4\pi r}, \quad (\nabla^2 + k^2)G(\mathbf{r}) = -\delta(\mathbf{r}), \quad r = |\mathbf{r}|. \tag{68}$$

Consider the representation of the field of the dipole (67) via scalar potentials (5). First we note that for the field (67) the function $\phi \equiv 0$ (as this function is determined up to an arbitrary function of the distance $r = |\mathbf{r}|$). This is not difficult to show, since we have from Eqs. (67) and (57):

$$\mathscr{D}_{rr}[\phi] = \mathbf{r} \cdot (\nabla \times \mathbf{E}) = \mathbf{r} \cdot (\nabla G \times \mathbf{p}) = \frac{1}{r}\frac{\partial G}{\partial r}\mathbf{r} \cdot (\mathbf{r} \times \mathbf{p}) = 0. \tag{69}$$

Eqs. (67) and (57) yield then

$$\mathscr{D}_{rr}[\psi] = \mathbf{r} \cdot \mathbf{E} = (\mathbf{r} \cdot \mathbf{p})G + \frac{1}{k^2}(\mathbf{r} \cdot \nabla)(\mathbf{p} \cdot \nabla G) = \frac{1}{k^2}\mathscr{D}_{\mathbf{r}\cdot\mathbf{p}}[G]. \tag{70}$$

In the basis of singular spherical functions $\{S_n^m(\mathbf{r})\}$ the function $G(\mathbf{r})$ is represented by expansion coefficients G_n^m:

$$G_n^m = \frac{\mathrm{i}k}{(4\pi)^{1/2}}\delta_{m0}\delta_{n0}, \quad n = 0, 1, \ldots, \quad m = -n, \ldots, n \quad \left(G(\mathbf{r}) = \frac{\mathrm{i}k}{(4\pi)^{1/2}}S_0^0(\mathbf{r}) = G_0^0 S_0^0(\mathbf{r})\right). \tag{71}$$

Representation (41) of operator $\mathscr{D}_{\mathbf{r}\cdot\mathbf{p}}$ shows then that for function $\mathscr{D}_{\mathbf{r}\cdot\mathbf{p}}[G]$ only expansion coefficients corresponding to degree $n = 1$ are non-zero, and, in fact, are dipoles for the scalar Helmholtz equation. So, using inversion (39) of operator $\mathbf{D}_{rr}$ we obtain

$$\psi_n^m = -\delta_{n1}\frac{1}{2k}\{(p_x + \mathrm{i}p_y)b_1^m G_0^{m+1} + (p_x - \mathrm{i}p_y)b_1^{-m} G_0^{m-1} - 2p_z a_0^m G_0^m\}, \quad n = 0, 1, \ldots, \quad m = -n, \ldots, n. \tag{72}$$

Inserting here expressions for differentiation coefficients (16) and (17) and for G_n^m (71) we obtain then the formulae for non-zero expansion coefficients of function ψ.

$$\psi_1^{-1} = \frac{p_y - \mathrm{i}p_x}{(24\pi)^{1/2}}, \quad \psi_1^0 = \frac{\mathrm{i}p_z}{(12\pi)^{1/2}}, \quad \psi_1^1 = \frac{p_y + \mathrm{i}p_x}{(24\pi)^{1/2}}. \tag{73}$$

Note, that the electric dipole can also be represented in the form:

$$\psi(\mathbf{r}) = -\frac{1}{k^2}\mathbf{p}\cdot\nabla G(\mathbf{r}). \tag{74}$$

This can be shown comparing Eqs. (72) and (18) to represent operator $\mathbf{p}\cdot\nabla$. One can also perform an exercise with vector algebra to show that $\nabla\times(\nabla\psi\times\mathbf{r}) = \mathbf{E}$ for ψ and $\mathbf{E}$ given by expressions (74) and (67). Taking into account (74) we can rewrite (67) in the form

$$\mathbf{E} = \mathbf{p}G - \nabla\psi. \tag{75}$$

Similar expressions can be obtained for fictitious point magnetic currents, where $\mathbf{H}(\mathbf{r})$ is represented in form (67). In this case we should have $\psi = 0$, while ϕ should be a sum of scalar dipoles with moments proportional to that given by Eq. (73).

5. Multiple scattering from spheres

To demonstrate how the method of scalar potentials can be efficiently applied for solution of scattering problems we will provide a solution of a classical problem of scattering off spheres (e.g. [4,20,28]). We also draw attention to a corresponding calculation for the scalar Helmholtz equation presented in [12]. This requires solution of a boundary value problem for Maxwell's equations. Assume that in general we have N dielectric spheres with radii a_q of electric permittivity ϵ_q and magnetic permeability μ_q respectively, and whose centers are located at $\mathbf{r}'_q$, $q = 1,\ldots,N$. In the absence of spheres the electromagnetic field is a given incident field, $(\mathbf{E}^{\mathrm{in}}, \mathbf{H}^{\mathrm{in}})$, while the presence of scatterers generates the scattered field $(\mathbf{E}^{\mathrm{scat}}, \mathbf{H}^{\mathrm{scat}})$, in the domain external to the spheres we have

$$\mathbf{E} = \mathbf{E}^{\mathrm{in}} + \mathbf{E}^{\mathrm{scat}}, \quad \mathbf{H} = \mathbf{H}^{\mathrm{in}} + \mathbf{H}^{\mathrm{scat}}, \tag{76}$$

and respective decomposition of scalar potentials ϕ and ψ.

On the surface of the qth scatterer, S_q, we have transmission conditions

$$(\mathbf{n}_q\times\mathbf{E})_{S_q} = (\mathbf{n}_q\times\mathbf{E}_q)_{S_q}, \quad (\mathbf{n}_q\times\mathbf{H})_{S_q} = (\mathbf{n}_q\times\mathbf{H}_q)_{S_q}, \tag{77}$$

where $\mathbf{n}_q$ is the surface normal, and $(\mathbf{E}_q, \mathbf{H}_q)$ is the electromagnetic field inside the qth scatterer.

5.1. Scattering from a single sphere

For a single sphere the electromagnetic scattering problem was considered by Mie [31], who provided a solution in the form of Mie series, i.e. series for electric and magnetic field vectors via vector spherical basis functions of type (12). Below we provide a solution of the same problem using scalar potentials.

5.1.1. Boundary conditions for scalar potentials

Consider a reference frame with the origin at the center of sphere of radius a. Denote $(\mathbf{E}^{\mathrm{int}}, \mathbf{H}^{\mathrm{int}})$ the field inside the sphere. Let then $\mathbf{E}$ and $\mathbf{E}^{\mathrm{int}}$ be represented in the form (5), (r,θ,φ) be the spherical coordinates, and

$$\begin{aligned} &\phi - \phi^{\mathrm{int}}|_{r=a} = \phi_a(\theta,\varphi), \quad \psi - \psi^{\mathrm{int}}|_{r=a} = \psi_a(\theta,\varphi),\\ &\left.\frac{\partial\phi}{\partial r}\right|_{r=a} - \left.\frac{\partial\phi^{\mathrm{int}}}{\partial r}\right|_{r=a} = \phi'_a(\theta,\varphi), \quad \left.\frac{\partial\psi}{\partial r}\right|_{r=a} - \left.\frac{\partial\psi^{\mathrm{int}}}{\partial r}\right|_{r=a} = \psi'_a(\theta,\varphi). \end{aligned} \tag{78}$$

Then we can express $\mathbf{n}\times(\mathbf{E} - \mathbf{E}^{\mathrm{int}})|_{r=a}$ via these functions and normal derivatives. Indeed, the first boundary condition (77) in terms of scalar potentials can be written as

$$\mathbf{r}\times\nabla\times(\mathbf{r}(\phi - \phi^{\mathrm{int}})) + \mathbf{r}\times\nabla\times\nabla\times(\mathbf{r}(\psi - \psi^{\mathrm{int}}))|_{r=a} = \mathbf{0}. \tag{79}$$

We have

$$\nabla\phi - \nabla\phi^{\text{int}}|_{r=a} = \phi'_a \mathbf{i}_r + \nabla\phi_a. \tag{80}$$

Since

$$\mathbf{r} \times \nabla \times (\mathbf{r}\phi) = \mathbf{r} \times (\nabla\phi \times \mathbf{r}) = r^2\nabla\phi - \mathbf{r}(\mathbf{r} \cdot \nabla\phi), \tag{81}$$

we obtain

$$\mathbf{r} \times \nabla \times (\mathbf{r}(\phi - \phi'))|_{r=a} = a^2(\phi'_a \mathbf{i}_r + \nabla\phi_a) - a^2\phi'_a \mathbf{i}_r = a^2\nabla\phi_a. \tag{82}$$

Then we have

$$\begin{aligned}\nabla(\psi + \mathbf{r} \cdot \nabla\psi)|_{r=a} &= \mathbf{i}_r \frac{\partial}{\partial r}\left(\psi + r\frac{\partial\psi}{\partial r}\right) + \frac{1}{r}\mathbf{i}_\theta \frac{\partial}{\partial\theta}\left(\psi + r\frac{\partial\psi}{\partial r}\right) + \frac{1}{r\sin\theta}\mathbf{i}_\varphi \frac{\partial}{\partial\varphi}\left(\psi + r\frac{\partial\psi}{\partial r}\right)\Bigg|_{r=a} \\ &= \mathbf{i}_r \frac{\partial}{\partial r}\left(\psi + r\frac{\partial\psi}{\partial r}\right)\Bigg|_{r=a} + \nabla\left(\psi + a\frac{\partial\psi}{\partial r}\Bigg|_{r=a}\right).\end{aligned} \tag{83}$$

So, using the first vector identity from Eq. (29) we obtain

$$\mathbf{r} \times \nabla \times \nabla \times (\mathbf{r}(\psi - \psi'))|_{r=a} = a\mathbf{i}_r \times \nabla(\psi_a + a\psi'_a). \tag{84}$$

We can rewrite the boundary conditions then as

$$a\nabla\phi_a + \mathbf{i}_r \times \nabla(\psi_a + a\psi'_a) = 0. \tag{85}$$

Since for spherical basis vectors we have $\mathbf{i}_r \times \mathbf{i}_\theta = \mathbf{i}_\varphi$, $\mathbf{i}_r \times \mathbf{i}_\varphi = -\mathbf{i}_\theta$ the above relation can be rewritten in component form as

$$a\sin\theta\frac{\partial\phi_a}{\partial\theta} = \frac{\partial}{\partial\varphi}(\psi_a + a\psi'_a), \quad \frac{a}{\sin\theta}\frac{\partial\phi_a}{\partial\varphi} = -\frac{\partial}{\partial\theta}(\psi_a + a\psi'_a). \tag{86}$$

We can then separate ϕ and ψ by cross-differentiation:

$$\begin{aligned}&\frac{\partial}{\partial\varphi}\left(\frac{1}{\sin\theta}\frac{\partial\phi_a}{\partial\varphi}\right) + \frac{\partial}{\partial\theta}\left(\sin\theta\frac{\partial\phi_a}{\partial\theta}\right) = 0, \\ &\frac{\partial}{\partial\varphi}\left(\frac{1}{\sin\theta}\frac{\partial}{\partial\varphi}(\psi_a + a\psi'_a)\right) + \frac{\partial}{\partial\theta}\left(\sin\theta\frac{\partial}{\partial\theta}(\psi_a + a\psi'_a)\right) = 0.\end{aligned} \tag{87}$$

The Beltrami operator is

$$\nabla^2_{(\theta,\varphi)} = \frac{1}{\sin\theta}\frac{\partial}{\partial\theta}\left(\sin\theta\frac{\partial}{\partial\theta}\right) + \frac{1}{\sin^2\theta}\frac{\partial^2}{\partial\varphi^2}. \tag{88}$$

So we obtain

$$\nabla^2_{(\theta,\varphi)}\phi_a = 0, \quad \nabla^2_{(\theta,\varphi)}(\psi_a + a\psi'_a) = 0. \tag{89}$$

The spherical harmonics $Y_n^m(\theta,\varphi)$ are eigenfunctions of the Beltrami operator with eigenvalues $-n(n+1)$. Hence, we have equalizing to zero each harmonic (excluding zero):

$$\phi_a|_{r=a} = 0, \quad \psi_a + a\psi'_a = 0, \tag{90}$$

or

$$\phi|_{r=a} = \phi^{\text{int}}|_{r=a}, \quad \left(\psi + a\frac{\partial\psi}{\partial r}\right)\Bigg|_{r=a} = \left(\psi^{\text{int}} + a\frac{\partial\psi^{\text{int}}}{\partial r}\right)\Bigg|_{r=a}. \tag{91}$$

Note that in case of perfect conductor the field inside the sphere is zero, and, therefore, the right hand sides of Eq. (91) should be set to zero.

Now we note that for dielectric spheres the same consideration applies to the vector of magnetic field, where the function ϕ should be replaced by $\frac{k^2}{\mathrm{i}\omega\mu}\psi$, while the function ψ should be replaced by $\frac{1}{\mathrm{i}\omega\mu}\phi$ (see (5)). From Eq. (91) we have then

$$\epsilon\psi|_{r=a} = \epsilon^{\text{int}}\psi^{\text{int}}|_{r=a}, \quad \frac{1}{\mu}\left(\phi + a\frac{\partial\phi}{\partial r}\right)\Big|_{r=a} = \frac{1}{\mu^{\text{int}}}\left(\phi^{\text{int}} + a\frac{\partial\phi^{\text{int}}}{\partial r}\right)\Big|_{r=a}, \tag{92}$$

where we noticed that for a given frequency

$$\frac{1}{c\mu k} = \frac{1}{\omega\mu}, \quad \frac{k^2}{\omega\mu} = \frac{\omega}{c^2\mu} = \omega\epsilon. \tag{93}$$

5.1.2. T-matrix

The T-matrix relates coefficients of the incident and scattered fields (e.g. see [24]). In terms of scalar potentials this relation can be found from the boundary conditions (91) and expansions of the scalar potentials over the spherical basis functions. Since the zero-order harmonics should be zero, these expansions are

$$\begin{aligned}
\phi^{\text{in}} &= \sum_{n=1}^{\infty}\sum_{m=-n}^{n}\phi_n^{(\text{in})m}R_n^m(\mathbf{r}), \quad \psi^{\text{in}} = \sum_{n=1}^{\infty}\sum_{m=-n}^{n}\psi_n^{(\text{in})m}R_n^m(\mathbf{r}),\\
\phi^{\text{scat}} &= \sum_{n=1}^{\infty}\sum_{m=-n}^{n}\phi_n^{(\text{scat})m}S_n^m(\mathbf{r}), \quad \psi^{\text{scat}} = \sum_{n=1}^{\infty}\sum_{m=-n}^{n}\psi_n^{(\text{scat})m}S_n^m(\mathbf{r}),\\
\phi^{\text{int}} &= \sum_{n=1}^{\infty}\sum_{m=-n}^{n}\phi_n^{(\text{int})m}R_n^m(v\mathbf{r}), \quad \psi^{\text{int}} = \sum_{n=1}^{\infty}\sum_{m=-n}^{n}\psi_n^{(\text{int})m}R_n^m(v\mathbf{r}), \quad v = \frac{k^{\text{int}}}{k},
\end{aligned} \tag{94}$$

where k^{int} is the wavenumber for the field inside the sphere, v is the relative refractive index.

Now we note that due to completeness and orthogonality of the spherical harmonics the relations for surface functions (91) apply to each harmonic independently. For each n and m this provides a system of four linear equations with respect to four unknowns $\phi_n^{(\text{scat})m}, \phi_n^{(\text{int})m}, \psi_n^{(\text{scat})m}, \psi_n^{(\text{int})m}$. To resolve the system in simpler form, we introduce the Ricatti–Bessel and Ricatti–Hankel functions

$$\eta_n(z) = zj_n(z), \quad \zeta_n(z) = zh_n(z). \tag{95}$$

In this case

$$\begin{aligned}
\phi_n^{(\text{scat})m} &= -\frac{v\eta_n(ka)\eta_n'(k^{\text{int}}a) - \frac{\mu^{\text{int}}}{\mu}\eta_n'(ka)\eta_n(k^{\text{int}}a)}{v\zeta_n(ka)\eta_n'(k^{\text{int}}a) - \frac{\mu^{\text{int}}}{\mu}\zeta_n'(ka)\eta_n(k^{\text{int}}a)}\phi_n^{(\text{in})m},\\
\psi_n^{(\text{scat})m} &= -\frac{v\eta_n(ka)\eta_n'(k^{\text{int}}a) - \frac{\epsilon^{\text{int}}}{\epsilon}\eta_n'(ka)\eta_n(k^{\text{int}}a)}{v\zeta_n(ka)\eta_n'(k^{\text{int}}a) - \frac{\epsilon^{\text{int}}}{\epsilon}\zeta_n'(ka)\eta_n(k^{\text{int}}a)}\psi_n^{(\text{in})m},\\
\phi_n^{(\text{int})m} &= v\frac{\mu^{\text{int}}}{\mu}\frac{\zeta_n(ka)\eta_n'(ka) - \zeta_n'(ka)\eta_n(ka)}{v\zeta_n(ka)\eta_n'(k^{\text{int}}a) - \frac{\mu^{\text{int}}}{\mu}\zeta_n'(ka)\eta_n(k^{\text{int}}a)}\phi_n^{(\text{in})m},\\
\psi_n^{(\text{int})m} &= v\frac{\zeta_n(ka)\eta_n'(ka) - \zeta_n'(ka)\eta_n(ka)}{v\zeta_n(ka)\eta_n'(k^{\text{int}}a) - \frac{\epsilon^{\text{int}}}{\epsilon}\zeta_n'(ka)\eta_n(k^{\text{int}}a)}\psi_n^{(\text{in})m}.
\end{aligned} \tag{96}$$

The coefficients relating $\phi_n^{(\text{scat})m}$ and $\phi_n^{(\text{int})m}$ to $\phi_n^{(\text{in})m}$ are the Lorenz–Mie coefficients for the TE partial wave polarization, and the coefficient relating $\psi_n^{(\text{scat})m}$ and $\psi_n^{(\text{int})m}$ to $\psi_n^{(\text{in})m}$ are the Lorenz–Mie coefficient for the TM partial wave polarization (in optics approximation $\mu^{\text{int}} = \mu$, $\epsilon^{\text{int}} = v^2\epsilon$ is usually employed – in this case the Lorenz–Mie coefficients depend only on ka and v).

Note that expressions for the internal field coefficients can be simplified using the Wronskian for spherical Bessel functions

$$\begin{aligned}
\zeta_n(ka)\eta_n'(ka) - \zeta_n'(ka)\eta_n(ka) &= ka\{h_n(ka)[j_n(ka) + kaj_n'(ka)] - [h_n(ka) + kah_n'(ka)]j_n(ka)\}\\
&= (ka)^2[h_n(ka)j_n'(ka) - h_n'(ka)j_n(ka)] = -i.
\end{aligned} \tag{97}$$

So

$$\phi_n^{(\mathrm{int})m} = -\mathrm{i}v\frac{\mu^{\mathrm{int}}}{\mu}\left(v\zeta_n(ka)\eta_n'(k^{\mathrm{int}}a) - \frac{\mu^{\mathrm{int}}}{\mu}\zeta_n'(ka)\eta_n(k^{\mathrm{int}}a)\right)^{-1}\phi_n^{(\mathrm{in})m},$$
$$\psi_n^{(\mathrm{int})m} = -\mathrm{i}v\left(v\zeta_n(ka)\eta_n'(k^{\mathrm{int}}a) - \frac{\epsilon^{\mathrm{int}}}{\epsilon}\zeta_n'(ka)\eta_n(k^{\mathrm{int}}a)\right)^{-1}\psi_n^{(\mathrm{in})m}. \tag{98}$$

We checked that the obtained solution coincides with the Mie solution. For this purpose we took the incident field in the form of plane wave (58) and found expansion coefficients for corresponding scalar potentials using Eqs. (63) and (66). Further we computed coefficients the Lorenz–Mie coefficients and determined the expansion coefficients for the scalar potentials of the scattered field according to Eq. (96). Evaluation of the scattered electric and magnetic fields was performed using truncated expansions of the x, y, and z field components over the singular spherical basis functions, where the expansion coefficients were computed using Eq. (55).

5.1.3. Error bounds

In computations we truncate all series for ϕ and ψ up to the degree $n = p - 1$. The error due to such a truncation can be estimated as follows. We note that the truncated solution satisfies Maxwell's equations, the scattered field is radiating, and the only deficiency is the error in the boundary conditions on the scatterer surface. As the complex amplitudes for all modes up to $n = p - 1$ are exact, while the modes of the scattered and the internal fields are zero for $n \geqslant p$ the error is only due to the boundary values of the incident field for modes $n \geqslant p$. Function $\mathbf{E}^{(\mathrm{in})}$ on the scatterer surface can be represented in the form

$$\mathbf{E}^{(\mathrm{in})}|_{r=a} = \sum_{n=1}^{\infty}\mathbf{E}_n^{(\mathrm{in})}(\mathbf{s}')j_n(ka), \quad \mathbf{E}_n^{(\mathrm{in})}(\mathbf{s}') = \sum_{m=-n}^{n}\mathbf{E}_n^{(\mathrm{in})m}Y_n^m(\mathbf{s}'), \quad \mathbf{r} = r\mathbf{s}', \quad |\mathbf{s}'| = 1. \tag{99}$$

The magnitudes of the surface functions $\mathbf{E}_n^{(\mathrm{in})}(\mathbf{s})$ are proportional to the amplitude of the incident field. Consider a typical field, e.g. a unit amplitude ($|\mathbf{q}| = 1$) incident plane wave (58), for which we have using (60)

$$|\mathbf{E}_n^{(\mathrm{in})}(\mathbf{s}')| = \left|4\pi(\mathbf{s}\times\mathbf{q})i^n\sum_{m=-n}^{n}Y_n^{-m}(\mathbf{s})Y_n^m(\mathbf{s}')\right| = |(2n+1)(\mathbf{s}\times\mathbf{q})i^nP_n(\mathbf{s}\cdot\mathbf{s}')| \leqslant 2n+1, \tag{100}$$

where P_n are the Legendre polynomials and we used the addition theorem for spherical harmonics, $|P_n| \leqslant 1$, and $|\mathbf{s}\times\mathbf{q}| = 1$. The truncation error then is bounded as

$$|\boldsymbol{\epsilon}_p| = \left|\sum_{n=p}^{\infty}\mathbf{E}_n^{(\mathrm{in})}(\mathbf{s}')j_n(ka)\right| \leqslant \sum_{n=p}^{\infty}|\mathbf{E}_n^{(\mathrm{in})}(\mathbf{s}')||j_n(ka)| \leqslant \sum_{n=p}^{\infty}(2n+1)|j_n(ka)|. \tag{101}$$

Because of $|\,j_n(ka)\,| \leqslant (ka)^n/[(2n+1)!!]$, [1], these series can be generally bounded as

$$|\boldsymbol{\epsilon}_p| \leqslant \sum_{n=p}^{\infty}\frac{(ka)^n}{(2n-1)!!} < \left(\frac{ka}{2}\right)\sum_{n=p-1}^{\infty}\frac{(ka)^n}{2^n n!} = \frac{\mathrm{e}^{ka/2}}{(p-1)!}\left(\frac{ka}{2}\right)^p, \tag{102}$$

since the latter sum can be treated as the residual term of the Taylor series for the exponent and bounded by Cauchy's formula. Even though this result is formally valid for any ka and, in fact, it shows that the series converges absolutely and uniformly, as $|\boldsymbol{\epsilon}_p| \to 0$ at $ka \to \infty$, the practical value of this estimate is for low and moderate ka. Indeed the term in the right hand side of Eq. (102) decays only for $p > eka/2$, while for $ka \gg 1$ a tighter bound can be established.

This follows from the fact that the spherical Bessel functions $j_n(ka)$ decay exponentially as functions of $\eta_n^{(a)} = (ka)^{-1/3}(n - ka + 1/2)$. An analysis of this decay can be found, e.g. in [14] (pp. 427–430), which yields for $\eta_n \gg 1$ (in fact the large η asymptotics are realized already at moderate values of η_n like $\eta_n \gtrsim 2$, see [14]) the following estimate

$$|\boldsymbol{\epsilon}_p| \lesssim (2p+1)|j_p(ka)| \lesssim \frac{p^{2/3}}{(ka)^{1/2}}\exp\left(-\frac{1}{3}(2\eta_p^{(a)})^{3/2}\right), \quad \eta_p^{(a)} = \frac{p - ka + 1/2}{(ka)^{1/3}}. \tag{103}$$

For high frequencies, $ka \gg 1$, $p \sim ka$, and prescribed $|\epsilon_p| = \epsilon$ we can determine then

$$p \gtrsim ka + \frac{1}{2}\left(3\ln\frac{1}{\epsilon} + \frac{1}{2}\ln(ka)\right)^{2/3}(ka)^{1/3}, \quad ka \gg 1. \tag{104}$$

Note that the term proportional to $\ln(ka)$ can usually be dropped (at $\epsilon ka \ll 1$ and due to small numerical coefficient) Such type of dependences and approximations based on them can be found in literature (e.g. [7]). Obviously the same analysis applies to the magnetic field.

5.2. Scattering from several spheres

To check the derived translation relations we considered the problem of scattering from several spheres. Solution of this problem for scalar case (acoustic scattering) using multipole reexpansions was obtained in Ref. [12] and, e.g. in Ref. [20] for the EM case. In the EM case it is convenient to use two component vectors for representation of expansion coefficients, where the first component corresponds to the potential ϕ and the second to the potential ψ. For scatterer q we can write then

$$\begin{pmatrix} \mathbf{\Phi}_q^{\text{scat}} \\ \mathbf{\Psi}_q^{\text{scat}} \end{pmatrix} = \begin{pmatrix} \mathbf{T}_q^{(\phi)} & \mathbf{0} \\ \mathbf{0} & \mathbf{T}_q^{(\psi)} \end{pmatrix} \begin{pmatrix} \mathbf{\Phi}_q^{\text{in,eff}} \\ \mathbf{\Psi}_q^{\text{in,eff}} \end{pmatrix}, \tag{105}$$

where $\mathbf{T}_q^{(\phi)}$ and $\mathbf{T}_q^{(\psi)}$ are diagonal matrices of Lorenz–Mie coefficients (T-matrices) for the qth scatterer, while $\mathbf{\Phi}_q^{\text{in,eff}}$ and $\mathbf{\Psi}_q^{\text{in,eff}}$ are the coefficients of the effective incident field for this scatterer. The latter coefficients can be thought as a sum of coefficients for the actual incident field (e.g. taken in the form of plane wave) and coefficients due to other scatterers. So we can write

$$\begin{pmatrix} \mathbf{\Phi}_q^{\text{in,eff}} \\ \mathbf{\Psi}_q^{\text{in,eff}} \end{pmatrix} = \begin{pmatrix} \mathbf{\Phi}_q^{\text{in}} \\ \mathbf{\Psi}_q^{\text{in}} \end{pmatrix} + \sum_{q' \neq q} \begin{pmatrix} \mathbf{C}_{11}(\mathbf{r}'_{q'q}) & k^2\mathbf{C}_{21}(\mathbf{r}'_{q'q}) \\ \mathbf{C}_{21}(\mathbf{r}'_{q'q}) & \mathbf{C}_{11}(\mathbf{r}'_{q'q}) \end{pmatrix} \times \begin{pmatrix} (\mathbf{S}|\mathbf{R})(\mathbf{r}'_{q'q}) & \mathbf{0} \\ \mathbf{0} & (\mathbf{S}|\mathbf{R})(\mathbf{r}'_{q'q}) \end{pmatrix} \begin{pmatrix} \mathbf{\Phi}_{q'}^{\text{scat}} \\ \mathbf{\Psi}_{q'}^{\text{scat}} \end{pmatrix}, \tag{106}$$

where $\mathbf{r}'_{q'q} = \mathbf{r}'_q - \mathbf{r}'_{q'}$ is a vector directed from the center of scatterer q' to scatterer q and we used representation of the translation operator in form (47) with multipole-to-local $(\mathbf{S}|\mathbf{R})$ translation operator.

One can substitute Eq. (106) into Eq. (105) to obtain a linear system of type

$$\mathbf{L}\mathbf{A} = \mathbf{A}^{\text{in}}, \quad \mathbf{L} = \mathbf{T}^{-1} - \widetilde{(\mathbf{S}|\mathbf{R})}, \tag{107}$$

where $\mathbf{A}$ is a vector stacking expansion coefficients $(\mathbf{\Phi}_q^{\text{scat}}, \mathbf{\Psi}_q^{\text{scat}}), q = 1, \ldots, N$, $\mathbf{A}^{\text{in}}$ is the vector of incident field coefficients, $\mathbf{T}$ is the diagonal T-matrix composed of $\mathbf{T}_q^{(\phi)}$ and $\mathbf{T}_q^{(\psi)}, q = 1, \ldots, N$, and $\widetilde{(\mathbf{S}|\mathbf{R})}$ denotes translation operator, which is composed from blocks of scalar translation operators and conversion matrices. This system can be solved directly using standard methods. In practice, we use truncation of the vectors and matrices with truncation number p to have p^2 expansion coefficients for each scatterer. This results in the system of size $2Np^2$. Computation of entries of the translation matrices takes $\mathrm{O}(N^2p^4)$ operations and direct solution (e.g. using Gauss elimination or LU-decomposition) can be done in $\mathrm{O}((Np^2)^3)$ operations. This complexity prevents one from solving problems with large N and p and some other methods should be used in this case. For example, the computational work can be reduced via an iterative method to $\mathrm{O}(N^2p^3N_{\text{iter}})$, where N_{iter} is the number of iterations, if we use the rotation-coaxial translation decomposition. Indeed in this case each iteration requires just one matrix–vector multiplication involving the system matrix $\mathbf{L}$. As Eq. (107) shows, this consists of diagonal $(\mathbf{T}^{-1})$ matrix multiplication and multiplication by the matrix $\widetilde{(\mathbf{S}|\mathbf{R})}$. The latter operation can be performed for expense of $(2N)^2p^3$ operations, if instead of (47) we use the decomposition (49). This method works well for $N \lesssim 100$, while for larger N methods for matrix–vector multiplication linear with respect to N (or $N\log N$), such as fast multipole methods (e.g. see [7,19,14,15]) or other speed up techniques [25] must be employed. We do not consider such techniques in this paper.

5.2.1. Error bounds

For the case of multiple scatterers the idea of the error estimation is the same as for a single scatterer with the remark that the effective, not actual, incident field is truncated. This field is a superposition of two fields: the true incident field (e.g. a plane wave) for which the error can be estimated as for a single scatterer (see Eq. (101)), and truncation of the high degree modes of each scattered field, $\mathbf{E}^{\mathrm{scat},q'}(\mathbf{r}), q' = 1,\ldots,N, q' \neq q$, reexpanded about the center of the given scatterer q. Despite the fact that each of these fields consists of $p-1$ modes of n,

$$\mathbf{E}^{\mathrm{scat},q'}(\mathbf{r}) = \sum_{n=1}^{p-1}\sum_{m=-n}^{n} \mathbf{E}_n^{(\mathrm{scat},q')m} S_n^m(\mathbf{r} - \mathbf{r}'_{q'}), \tag{108}$$

the translated expansion will contain an infinite number of modes, as we have

$$\begin{aligned} \mathbf{E}^{\mathrm{scat},q'}(\mathbf{r}) &= \sum_{n=1}^{\infty}\sum_{m=-n}^{n} \widehat{\mathbf{E}}_n^{(\mathrm{scat},q')m} R_n^m(\mathbf{r} - \mathbf{r}'_q), \\ \widehat{\mathbf{E}}_n^{(\mathrm{scat},q')m} &= \sum_{n'=1}^{p-1}\sum_{m'=-n'}^{n'} (S|R)_{nn'}^{mm'}(\mathbf{r}'_{q'q}) \mathbf{E}_{n'}^{(\mathrm{scat},q')m'}, \quad n = 1,2,\ldots \end{aligned} \tag{109}$$

If the truncated linear system is solved exactly, then the first $p-1$ modes for these series are determined exactly, and the error in the electric field on the boundary of scatterer q will be

$$\begin{aligned} |\boldsymbol{\epsilon}_p^{(q)}| &= |\boldsymbol{\epsilon}_p^{\mathrm{in}(q)} + \sum_{q'\neq q} \boldsymbol{\epsilon}_p^{(q'q)}| \leqslant |\boldsymbol{\epsilon}_p^{\mathrm{in}(q)}| + \sum_{q'\neq q} |\boldsymbol{\epsilon}_p^{(q'q)}|, \\ \boldsymbol{\epsilon}_p^{(q'q)} &= \sum_{n=p}^{\infty}\sum_{m=-n}^{n} \widehat{\mathbf{E}}_n^{(\mathrm{scat},q')m} R_n^m(\mathbf{r} - \mathbf{r}'_q), \quad |\mathbf{r} - \mathbf{r}'_q| = a_q, \end{aligned} \tag{110}$$

where $|\boldsymbol{\epsilon}_p^{\mathrm{in}(q)}|$ is the magnitude of the error due to the incident field truncation (101).

To evaluate this error we introduce surface function for mode n of each scatterer

$$\mathbf{E}_n^{(\mathrm{scat},q')}(\mathbf{s}') = \sum_{m=-n}^{n} \mathbf{E}_n^{(\mathrm{scat},q')m} Y_n^m(\mathbf{s}'), \quad |\mathbf{s}'| = 1, \quad n = 1,2,\ldots, \quad q' = 1,\ldots,N. \tag{111}$$

The translation errors $\boldsymbol{\epsilon}_p^{(q'q)}$ now can be estimated using the technique developed in Ref. [14]. For this purpose we combine Eqs. (109) and (110) to have:

$$\begin{aligned} |\boldsymbol{\epsilon}_p^{(q'q)}| &= \left|\sum_{n'=1}^{p-1} \boldsymbol{\delta}_{n'}^{(q'q)}\right| \leqslant \sum_{n'=1}^{p-1} |\boldsymbol{\delta}_{n'}^{(q'q)}|, \\ \boldsymbol{\delta}_{n'}^{(q'q)} &= \sum_{n=p}^{\infty} j_n(ka_q) \sum_{m=-n}^{n}\sum_{m'=-n'}^{n'} (S|R)_{nn'}^{mm'}(\mathbf{r}'_{q'q}) \mathbf{E}_{n'}^{(\mathrm{scat},q')m'} Y_n^m(\mathbf{s}'), \quad \mathbf{r} - \mathbf{r}'_q = a_q\mathbf{s}'. \end{aligned} \tag{112}$$

The following error bound then holds (see Appendix B):

$$\begin{aligned} |\boldsymbol{\delta}_{n'}^{(q'q)}| &< (2n'+1)\alpha_{n'} \max_{\mathbf{s}'} |\mathbf{E}_{n'}^{(\mathrm{scat},q')}(\mathbf{s}')| \epsilon_p^{s(q'q)}, \quad \epsilon_p^{s(q'q)} = \sum_{n=p}^{\infty} (2n+1)|j_n(ka_q)||h_n(kb_{q'q})|, \\ \alpha_{n'} &= \begin{cases} 1, & n' \leqslant ka_{q'} \\ \left(\frac{e\pi}{2n'-1}\right)^{1/2} |j_{n'}(ka_{q'})|^{-1}, & n' > ka_{q'}, \end{cases} \qquad b_{q'q} = r_{q'q} - a_{q'}. \end{aligned} \tag{113}$$

Note then that $\epsilon_p^{s(q'q)}$ is nothing, but a uniform bound for the truncation error of the multipole expansion about the center of scatterer q of the monopole source located at the closest to scatterer q point on the surface of scatterer q' and evaluated at the surface of scatterer q:

$$h_0(k(b_{q'q} - a_q)) = \sum_{n=0}^{\infty} (2n+1) j_n(ka_q) h_n(kb_{q'q}). \tag{114}$$

Function $\epsilon_p^{s(q'q)}$ which is the residual term of the Gegenbauer series has been studied in detail in the literature (e.g. Refs. [9,14]), where both strong bounds and approximations, which are closer to the computational results, are established. Particularly it was found in Ref. [14] that for moderate spacings between the spheres the relation between $\epsilon_p^{s(q'q)}$ and p can be well approximated by

$$p = \left\{ \left[\frac{1}{\ln \delta_{q'q}} \ln \frac{\delta_{q'q}^{3/2}}{\epsilon_p^{s(q'q)} ka_q (\delta_{q'q}-1)^{3/2}} + 1 \right]^4 + \left[ka_q + \frac{1}{2} \left(3 \ln \frac{1}{\epsilon_p^{s(q'q)} \delta} \right)^{2/3} (ka_q)^{1/3} \right]^4 \right\}, \qquad \delta_{q'q} = \frac{b_{q'q}}{a_q}. \tag{115}$$

For the present analysis, however, we need to express $\epsilon_p^{s(q'q)}$ via p, for which purpose this formula is not so convenient. So in Appendix B we derived the following approximation:

$$\epsilon_p^{s(q'q)} \lesssim \frac{p^{1/3}}{\delta_{q'q}^{1/2} ka_q} \exp\left\{ -\frac{1}{3} \left((2\eta_p^{(a)})^{3/2} - (2\eta_p^{(b)})^{3/2} \right) \right\},$$
$$\eta_p^{(b)} = \begin{cases} (kb_{q'q})^{-1/3} (p - kb_{q'q} + 1/2), & p > kb_{q'q} - 1/2 \\ 0, & p \leqslant kb_{q'q} - 1/2, \end{cases} \qquad \eta_p^{(a)} = \frac{p - ka_q + 1/2}{(ka_q)^{1/3}}. \tag{116}$$

We note then that $|j_n(ka_q)|$ exponentially decays for $n > ka_q$, while $|h_n(kb_{q'q})|$ exponentially grows for $n > kb_{q'q}$, as functions of n. The characteristic scale for the decay region of $|j_n(ka_q)|$ is $n - ka_q \sim (ka_q)^{1/3}$. Therefore, if $kb_{q'q} - ka_q \sim (ka_q)^{1/3}$ the rate of exponential convergence slows down and the truncation number increases substantially to provide the same error. Putting here $b_{q'q} = \delta_{q'q} a_q$ we can determine that this happens if $\delta_{q'q} - 1 \sim (ka_q)^{-2/3}$, in which case Eq. (116) provides for $ka_q \gg 1$

$$\epsilon_p^{s(q'q)} \lesssim \frac{p^{1/3}}{ka_q} \exp(-(\delta_{q'q}-1)(2ka_q)^{1/2}(p + 1/2 - ka_q)^{1/2}), \quad \delta_{q'q} - 1 \sim (ka_q)^{-2/3} \ll 1, \tag{117}$$

which provides the characteristic scale for the decay region: $n - ka_q \sim (\delta_{q'q}-1)^{-2}(ka_q)^{-1}$. This shows that the error cannot be bounded for $\delta_{q'q} = 1$, which can also be seen from its definition (113) as $|j_n(ka_q)||h_n(ka_q)| \sim n^{-1}$, $n \gg ka_q$, and the series diverges. In fact, numerical tests show that even for the case of touching spheres at sufficiently large p the error on the boundary tends to zero, except at the touching point [15], where in any case the normal to the joint sphere surface is not defined. However, to prove or disprove that a more involved technique is required, as in the present case we bounded the error uniformly on the surface. We also mention that the increase of the error as $\delta_{q'q}$ decreases has a clear meaning that more modes are required to represent the field of the scatterer q' via spherical harmonics centered at q as the distance between them decreases.

Further we note that absolute and uniform convergence of series (108) on the surface of scatterer q' requires

$$\max_{\mathbf{s}'} |\mathbf{E}_{n'}^{(\mathrm{scat},q')}(\mathbf{s}')| = \mathrm{o}(|n' h_{n'}(ka_{q'})|^{-1}), \quad n' \to \infty.$$

Since $n'|j_{n'}(ka_q)||h_{n'}(ka_q)| = \mathrm{O}(1)$ for $n' > ka_{q'}$ we obtain from Eq. (113):

$$|\boldsymbol{\delta}_{n'}^{(q'q)}| = \epsilon_p^{s(q'q)} \mathrm{o}((n')^{1/2}), \quad n' > ka_{q'}. \tag{118}$$

Hence substituting Eqs. (118) and (113) into finite sum (112) and assuming $p - ka_{q'} \sim (ka_{q'})^{1/3} \sim p^{1/3}$, we obtain

$$|\boldsymbol{\epsilon}_p^{(q'q)}| \leqslant \sum_{n'=1}^{p-1} |\boldsymbol{\delta}_{n'}^{(q'q)}| = \sum_{n'=1}^{[ka_{q'}]} |\boldsymbol{\delta}_{n'}^{(q'q)}| + \sum_{n'=[ka_{q'}]}^{p-1} |\boldsymbol{\delta}_{n'}^{(q'q)}| \lesssim \epsilon_p^{s(q'q)} [E_{\max}^{(\mathrm{scat},q')} (ka_{q'})^2 + \mathrm{o}((ka_{q'})^{5/6})] \sim E_{\max}^{(\mathrm{scat},q')} (ka_{q'})^2 \epsilon_p^{s(q'q)}, \tag{119}$$

where

$$E_{\max}^{(\mathrm{scat},q')} = \max_{n'} \max_{\mathbf{s}'} |\mathbf{E}_{n'}^{(\mathrm{scat},q')}(\mathbf{s}')|, \quad n' \leqslant ka_{q'}. \tag{120}$$

From Eqs. (110) and (119) we can obtain the following bound for the N sphere case

$$|\epsilon_p^{(q)}| \leqslant |\epsilon_p^{\mathrm{in}(q)}| + \sum_{q' \neq q} E_{\max}^{(\mathrm{scat},q')} (ka_{q'})^2 \epsilon_p^{s(q'q)} \leqslant |\epsilon_p^{\mathrm{in}(q)}| + (N-1) E_{\max}^{(\mathrm{scat})} (ka_{\max})^2 \epsilon_{p,\max}^{s(q)}, \tag{121}$$

where $E_{\max}^{(\mathrm{scat})}$, $a_{\max}$, and $\epsilon_{p,\max}^{s(q)}$ are the maximum values of these parameters over all scatterers. We note that error $\epsilon_p^{s(q'q)}$ substantially depends on the spacing between the scatterers and is much larger for neighbor scatterers if there are many scatterers in the field. So for large N a more accurate bound than (121) can be obtained, which treats the neighbor and remote scatterers differently. In the case of two equal spheres of radius a with separation parameter $\delta = b/a$ exposed to a plane wave we have according to Eqs. (121), (116), and (103)

$$|\epsilon_p^{(1)}| \sim |\epsilon_p^{(2)}| \lesssim \left[\frac{p^{2/3}}{(ka)^{1/2}} + C \frac{p^{1/3} ka}{\delta^{1/2}} \exp\left(\frac{1}{3} (2\eta_p^{(b)})^{3/2} \right) \right] \exp\left(-\frac{1}{3} (2\eta_p^{(a)})^{3/2} \right), \tag{122}$$

where C is some constant of order 1.

Finally we note that in the bounds obtained for components of the electric or magnetic field p should be increased by 1 to get bounds for the Debye potentials, as the $n+1$th mode of ϕ and ψ is required to obtain the nth mode of $\mathbf{E}$ and $\mathbf{H}$.

5.3. Numerical tests

In numerical tests we performed computations of scattering off a spatial distributions of N scatterers of equal or different size. The truncation number p was selected according to

$$p = [ka_{\max}] + p_0(ka_{\max}, \epsilon, \delta), \tag{123}$$

where $[\,]$ denotes integer part, p_0 depends on the acceptable error of computation, ϵ, maximum sphere radius, $a_{\max} = \max\{a_q\}$, and separation between the spheres, $\delta = \min\{b_q/a_q\}$, where b_q is the distance from the center of sphere q to the closest point on the neighbor sphere ($\delta \geqslant 1$). Such dependences were studied for the scalar case [15], and in the present study we used these results as a guide for selection of p. Also we obtained theoretical error bounds for solution of the problem. However, for every computed case at some p we performed *a posteriori* error check, to ensure that the solution is correct and made a comparison with the theoretical predictions.

The basis for the *a posteriori* error check is the following. As ϕ and ψ satisfy the scalar Helmholtz equation, the expansion coefficients for components of the electric field (55) (and similarly for magnetic field) ensure that the EM field is divergence free. Therefore, all errors (truncation, round-off, iteration) are related to the boundary conditions alone. To check that the obtained fields are actually solutions of the boundary value problem for the Maxwell equation, we sampled the entire boundary (of all scatterers) with M points, $\mathbf{y}_m$, at which we computed the following errors for the boundary conditions for electric field

$$\epsilon_m^{(\mathrm{bc})} = \frac{|\mathbf{n}(\mathbf{y}_m) \times [\mathbf{E}(\mathbf{y}_m) - \mathbf{E}^{\mathrm{int}}(\mathbf{y}_m)]|}{\left(\frac{1}{M} \sum_m |\mathbf{E}(\mathbf{y}_m)|^2 \right)^{1/2}}, \quad \epsilon_\infty^{(\mathrm{bc})} = \max_m \epsilon_m^{(\mathrm{bc})}, \quad \epsilon_2^{(\mathrm{bc})} = \left[\frac{1}{M} \sum_m |\epsilon_m^{(\mathrm{bc})}|^2 \right]^{1/2}. \tag{124}$$

A similar error measure was computed for the magnetic field as well. All computations reported below were performed in double precision.

5.3.1. Single sphere

Scattering from a single sphere is classical Mie scattering case, which solutions are investigated thoroughly (see, e.g. [3]). We validated our computations by comparisons of some standard cases. As a benchmark case we considered scattering off a perfect conductor, in which case $\mathbf{E}^{\mathrm{int}} = \mathbf{0}$ and so instead of general boundary conditions (77) it is sufficient to use $\mathbf{n} \times \mathbf{E} = \mathbf{0}$. This also can be considered as a limiting case with $\epsilon_{\mathrm{int}} \to \infty$, $\mu_{\mathrm{int}} \to 0$. To measure the error we sampled the surface with a equiangular grid with respect to the spherical angles θ and φ and performed computations for a range of ka and corresponding values of the truncation numbers p. Some results of error measurements are shown in Fig. 1.

For computations we used an incident field in the form of plane wave (58), where the electric field vector had polarization direction $\mathbf{p} = \mathbf{s} \times \mathbf{q}$ (usually we directed axes to have $\mathbf{s} = (0, 0, 1)$, $\mathbf{p} = (1, 0, 0)$). Some example of computation of distribution of parameters on the scatterer surface is shown in Fig. 1(left). Here the arrows show the direction of the wave vector, $\mathbf{s}$, and of the polarization vector, $\mathbf{p}$. The plotted value is the dimensionless energy density of the electromagnetic field, $e = \frac{1}{2}(|\mathbf{E}|^2 + |\mathbf{H}|^2)$, where $\mathbf{E}$ and $\mathbf{H}$ are the dimensionless electric and magnetic vectors (set $\epsilon = \mu = 1$). Fig. 1(right) shows $\epsilon_\infty^{(\mathrm{bc})}$ defined by Eq. (124) for a 21×20 surface grid which we used for error measurement. This error depends on ka and p or p_0, which is defined by Eq. (123). The curves of constant $\epsilon_\infty^{(\mathrm{bc})}$ divide the (ka, p_0) plane into domains shown in shades of gray. We also plotted the dependence for usually recommended criterion for selection of $p(ka)$ (e.g. [2])

$$p = ka + 4(ka)^{1/3} + 3 \tag{125}$$

(one can determine p_0 from this using Eq. (123)). As the figure shows the error in boundary conditions in this case is somewhere between 10^{-6} and 10^{-4}, which also slightly depends on ka. We also checked error bounds (102) and (104) for the errors in range $|\epsilon_p| = 10^{-8} - 10^{-2}$ (only case $|\epsilon_p| = 10^{-2}$, which is typical, is plotted in Fig. 1) and found an excellent agreement of the computed results and with Eq. (102) for $ka \lesssim 1$. However at $ka \gg 1$ this substantially overestimates the actual error. On the other hand the high frequency asymptotics (104) underestimate the error at low ka, while show a satisfactory estimate at $ka \gg 1$ (they may slightly underestimate or overestimate the actual error). Also we found that Eq. (103) is a good approximation for all cases.

5.3.2. Two spheres

The case of two spheres is also important for validation of the results, since this introduces separation distance between the spheres as an additional parameter affecting the error. Also this case validates the translation theory and the iterative solver (GMRES), which we used in all the multisphere cases for solution of the resulting linear system, since this brings substantial speed ups due to the rotation-coaxial translation decomposition.

Fig. 2 demonstrates some results of computations for two perfectly conducting spheres of equal size. The picture on the right shows patterns of the dimensionless energy density for $ka = 10$ and dimensionless separation $\delta = 2$. Comparing these with that shown in Fig. 1 we can see that the influence of the second sphere is substantial and also orientation of the vector directed from one sphere to the other with respect to the wave vector $\mathbf{s}$ and polarization vector $\mathbf{p}$ is important. The chart on the right of Fig. 2 shows computations of the

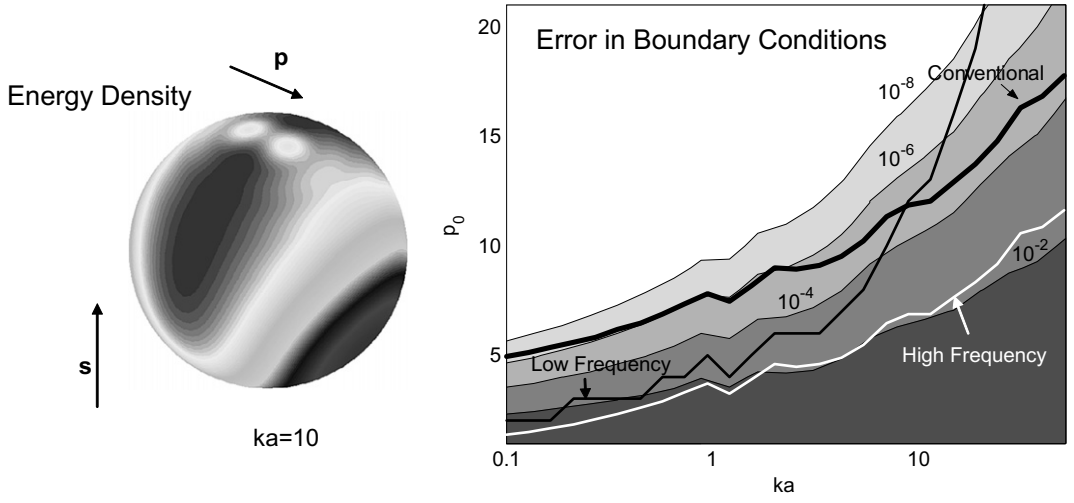

Fig. 1. On the left: the distribution of the dimensionless energy density over a surface of perfectly conducting sphere at $ka = 10$ for incident wave vector $\mathbf{s}$ and electric field polarization $\mathbf{p}$ shown. On the right: different shades of gray show areas of maximum relative error in boundary conditions $\epsilon_\infty^{(\mathrm{bc})}$ defined by Eq. (124), which is a function of ka and p_0. The thick curve shows conventional dependence (125) used by many authors. The thin curves correspond to Eq. (102) (black) and Eq. (104) (white) for $|\epsilon_p| = 10^{-2}$.

error in boundary conditions $\epsilon_\infty^{(bc)}$ as a function of p_0 and δ (measured for polarization shown in the left bottom picture for $ka = 5$). We can see that computations can be stably performed even for the case when the spheres touch each other ($\delta = 1$). However the truncation number in this case should be larger than predicted by Eq. (125) if the required accuracy is 10^{-4} or less. The increase in the truncation number for fixed accuracy depends on ka and δ as explained in the section related to the error bounds. We found then that Eq. (122) (we increased p by one as discussed) estimates the truncation numbers satisfactory for large and moderate $\delta - 1$ while overestimates p for $\delta - 1 < 1$. The possible reason for that is also mentioned earlier and related to the fact that Eq. (122) is derived based on a uniform bound of the mode magnitudes, while in reality the series converge for different points on the surface with different rates, which is especially true for close spheres. So the error obtained by surface sampling (124) is smaller than given by Eq. (122).

5.3.3. Multiple sphere cases

Many computations were performed for multiple sphere configurations, where we varied the sizes, locations, and dielectric properties of the spheres, the wave polarization directions and the wavenumber. Figs. 3 and 4 demonstrate some results for random and regular distributions of spheres with the same dielectric properties $\epsilon^{int}/\epsilon = 10 + 0.1i$, $\mu^{int}/\mu = 1$. In the first case the size distribution of the spheres was uniformly random with $a_{min}/a_{max} = 0.5$ and $ka_{max} = 10$. As the locations were also uniformly randomly generated inside some bounding box we removed overlapping spheres to leave 100 non-intersecting spheres (some of them were almost touching their neighbors). GMRES-based iteration process shows exponential convergence in terms of the absolute error in the expansion coefficients (see Fig. 3). After achieving some prescribed error the iteration process was terminated and the error in boundary conditions (124) was measured over 38,200 points sampling the entire surface of 100 spheres. As it is seen this error varies in a wide range, which we relate to the proximity of the neighbor spheres to a given one. If a sphere is well separated from the other spheres the error was low, and it substantially increases for touching spheres. In any case, the worst errors were of order of several percents in this case ($p = 26$).

The configuration shown in Fig. 4 is computed for a little bit higher wavenumbers and we used truncation number $p = 31$. Here the spheres of the same size are arranged in a grid with spacing equal to the sphere radius

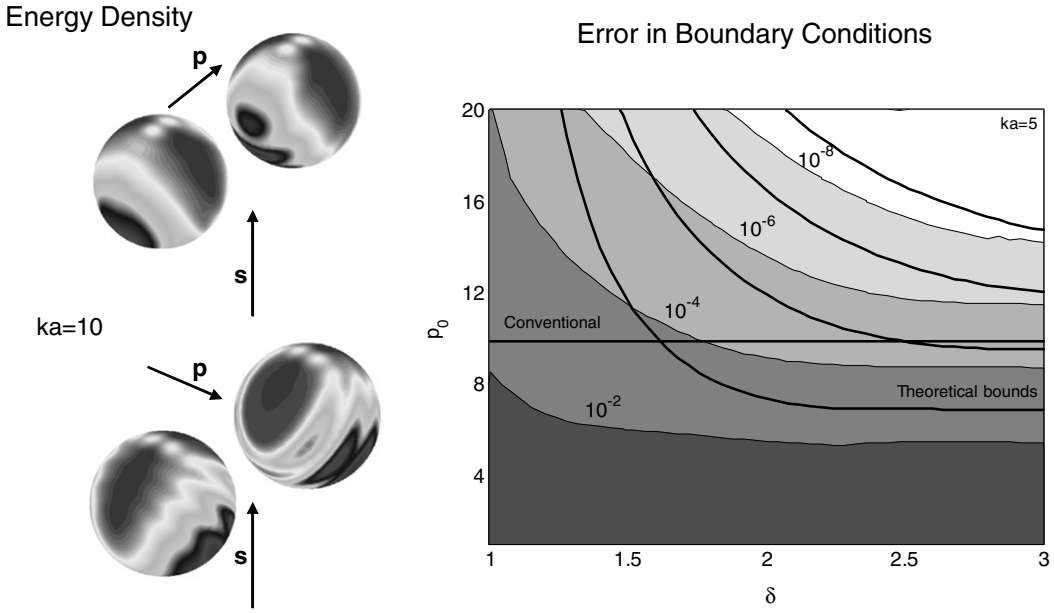

Fig. 2. Two pictures on the left illustrate distribution of the dimensionless field energy density over the surface of two perfect conductors at different polarizations of the incident plane wave shown by vector **p** at $ka = 10$. The graph on the right shows dependence of the error in boundary conditions $\epsilon_\infty^{(bc)}$ on the dimensionless separation parameter δ and p_0 for $ka = 5$. The solid horizontal line corresponds to Eq. (125) while the dotted curves are computed using Eq. (122) ($C = 1$) for prescribed $|\boldsymbol{\epsilon}_p^{(1)}| = |\boldsymbol{\epsilon}_p^{(2)}| = 10^{-8}, 10^{-6}, 10^{-4}$, and 10^{-2}, respectively.

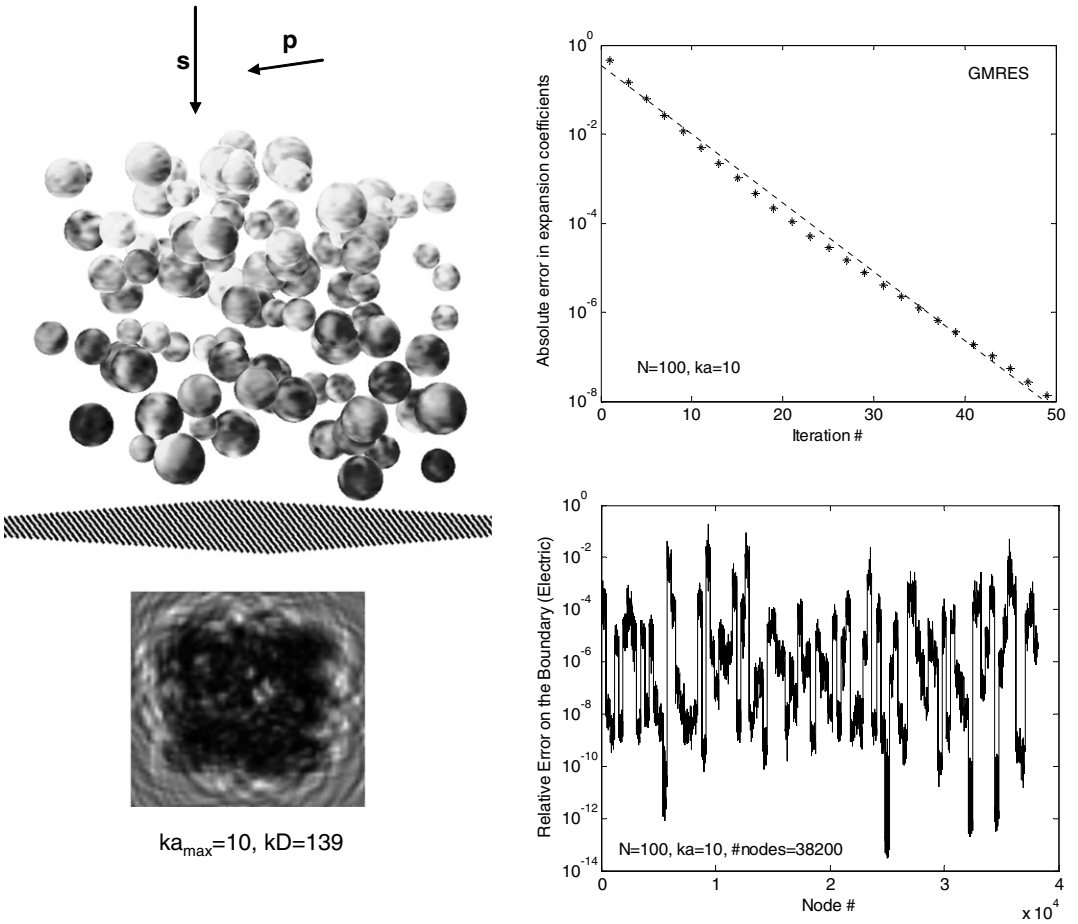

Fig. 3. Illustration of computations of scattering for 100 spheres of random size and location. The incident wave vector and polarization are shown by arrows **s** and **p**. Intensity of gray shadows on the spheres correspond to $\log_{10} e$, where e is the dimensionless energy density. The bottom left picture shows spatial distribution of e over the imaging plane represented by dots on the to left picture. The top right chart shows convergence of the GMRES-based iterative solver, and the bottom right chart illustrates distribution of error in boundary conditions ϵ_m (124) over 38,200 surface nodes.

($\delta = 2$). The nature of convergence of the iteration was the same as in the previous case, while the rate of convergence was a bit faster. The iterative process was terminated at about the same accuracy as in the case of random distribution, while the error in boundary conditions measured over 47 750 points which sampled the surface with the same density was substantially smaller and did not exceed 2.4×10^{-5}, which is because there were no spheres too close to each other in this case.

In any case these tests showed that the numerical process is stable and the error in the solution is reasonably small. Some additional research is obviously needed to improve the error for the cases when δ is close to 1 (while for comparison with experiments a few percent errors may be acceptable).

5.3.4. Computation of amplitude scattering matrix

The scattering matrix is introduced to handle cases of arbitrary wave polarization (due to the linearity of the scattering problem) and, therefore, does not depend on the polarization angle. If a group of scatterers is to be identified as a scattering object the amplitude scattering matrix can be computed. If we direct the z axis as the incident wave vector **s** and consider the scattering plane which passes through the z axis and the observation point, which is characterized by spherical coordinates (θ, φ) and is located far from the scatterer, then by definition the scattering matrix with components $S_1, \ldots, S_4$ that are functions of (θ, φ) relates components of the scattered far field and the incident field for electric vector as [2]

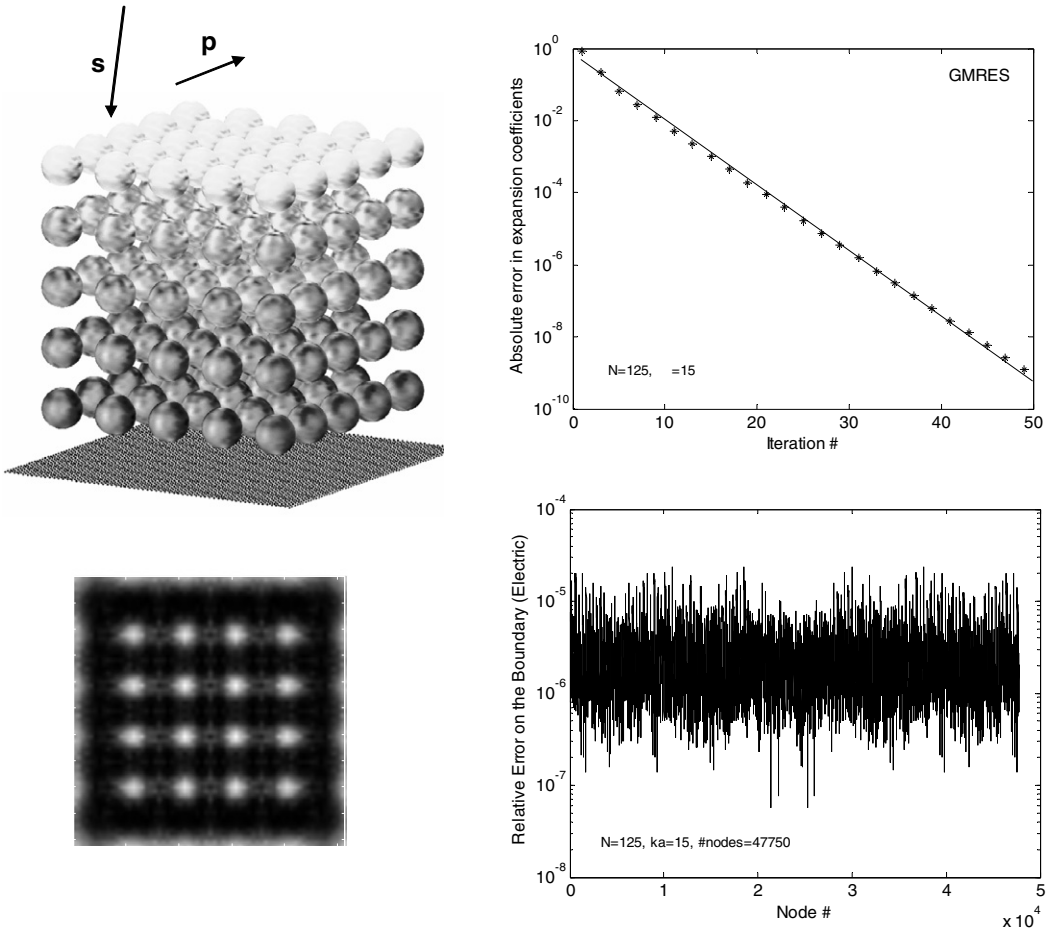

Fig. 4. The same as Fig. 3, but for a regular distribution of 125 spheres of equal size.

$$\begin{pmatrix} E_{\parallel}^{\text{scat}} \\ E_{\perp}^{\text{scat}} \end{pmatrix} = \frac{\mathrm{e}^{\mathrm{i}kr-\mathrm{i}kz}}{-\mathrm{i}kr} \begin{pmatrix} S_2 & S_3 \\ S_4 & S_1 \end{pmatrix} \begin{pmatrix} E_{\parallel}^{\text{in}} \\ E_{\perp}^{\text{in}} \end{pmatrix}, \tag{126}$$

where the symbols $\parallel$ and $\perp$ are related to the components parallel and perpendicular to the scattering plane.

The property of the far scattered field is that the radial component decays faster than the angular components, $E_r^{\text{scat}} = \mathrm{O}(r^{-2})$ (as $\mathbf{r} \cdot \mathbf{E}$ satisfies the Helmholtz equation), while $E_\theta^{\text{scat}} = \mathrm{O}(r^{-1})$, $E_\varphi^{\text{scat}} = \mathrm{O}(r^{-1})$. Therefore $E_{\parallel}^{\text{scat}} = E_\theta^{\text{scat}}$, and $E_{\perp}^{\text{scat}} = -E_\varphi^{\text{scat}}$. The parallel and perpendicular components of the incident field are related to the x and y components as

$$\begin{pmatrix} E_{\parallel}^{\text{in}} \\ E_{\perp}^{\text{in}} \end{pmatrix} = \begin{pmatrix} \cos\varphi & \sin\varphi \\ \sin\varphi & -\cos\varphi \end{pmatrix} \begin{pmatrix} E_x^{\text{in}} \\ E_y^{\text{in}} \end{pmatrix}, \tag{127}$$

while for the parallel and perpendicular components of the scattered field are

$$\begin{pmatrix} E_{\parallel}^{\text{scat}} \\ E_{\perp}^{\text{scat}} \end{pmatrix} = \begin{pmatrix} \cos\theta & 0 & -\sin\theta \\ 0 & 1 & 0 \end{pmatrix} \begin{pmatrix} \cos\varphi & \sin\varphi & 0 \\ \sin\varphi & -\cos\varphi & 0 \\ 0 & 0 & 1 \end{pmatrix} \begin{pmatrix} E_x^{\text{scat}} \\ E_y^{\text{scat}} \\ E_z^{\text{scat}} \end{pmatrix}. \tag{128}$$

In computations we can then solve two problems with x and y incident electric field polarization,

$$\mathbf{E}_x^{\text{in}} = (E_x^{\text{in}}, 0, 0)\mathrm{e}^{\mathrm{i}kz}, \quad \mathbf{E}_x^{\text{in}} = (0, E_y^{\text{in}}, 0)\mathrm{e}^{\mathrm{i}kz},$$

which produce vectors

$$\mathbf{E}_x^{\text{scat}} = (E_{xx}^{\text{scat}}, E_{xy}^{\text{scat}}, E_{xz}^{\text{scat}}), \quad \mathbf{E}_y^{\text{scat}} = (E_{yx}^{\text{scat}}, E_{yy}^{\text{scat}}, E_{yz}^{\text{scat}}),$$

respectively. Then, using Eqs. (126)–(128) we can derive

$$\begin{pmatrix} S_2 & S_3 \\ S_4 & S_1 \end{pmatrix} = \left(\frac{e^{ikr}}{-ikr}\right)^{-1} \begin{pmatrix} \cos\theta & 0 & -\sin\theta \\ 0 & 1 & 0 \end{pmatrix} \begin{pmatrix} \cos\varphi & \sin\varphi & 0 \\ \sin\varphi & -\cos\varphi & 0 \\ 0 & 0 & 1 \end{pmatrix} \begin{pmatrix} E_{xx}^{\text{scat}} & E_{yx}^{\text{scat}} \\ E_{xy}^{\text{scat}} & E_{yy}^{\text{scat}} \\ E_{xz}^{\text{scat}} & E_{yz}^{\text{scat}} \end{pmatrix} \begin{pmatrix} \cos\varphi & \sin\varphi \\ \sin\varphi & -\cos\varphi \end{pmatrix}. \tag{129}$$

Note then that the far-field pattern can be found from the computed expansion coefficients of scattered field related to $\phi_n^{(\text{scat})(q)m}$ and $\psi_n^{(\text{scat})(q)m}$ via (55) for each scatterer in the system of N scatterers:

$$\begin{aligned} \mathbf{E}^{\text{scat}}(\mathbf{r}) &= \sum_{q=1}^{N} \sum_{n=0}^{\infty} \sum_{m=-n}^{n} \mathbf{E}_n^{(\text{scat})(q)m} S_n^m(\mathbf{r} - \mathbf{r}_q') \sim \sum_{q=1}^{N} e^{-ik\mathbf{s}'\cdot\mathbf{r}_q'} \sum_{n=0}^{\infty} \sum_{m=-n}^{n} \mathbf{E}_n^{(\text{scat})(q)m} S_n^m(\mathbf{r}) \\ &\sim \frac{e^{ikr}}{ikr} \sum_{q=1}^{N} e^{-ik\mathbf{s}'\cdot\mathbf{r}_q'} \sum_{n=0}^{\infty} \sum_{m=-n}^{n} i^{-n} \mathbf{E}_n^{(q)(\text{scat})m} Y_n^m(\theta, \varphi), \\ \mathbf{s}' &= \frac{\mathbf{r}}{r} = (\sin\theta\cos\varphi, \sin\theta\sin\varphi, \cos\theta). \end{aligned} \tag{130}$$

Figs. 5 and 6 show some comparisons of computations using the present method with computations and experiments of Xu and Gustafson [30], which are well documented and data are available via their web site [30]. First we compared the computations for the two sphere configuration, where two identical touching spheres of optical BK7 glass (refractive index $k^{\text{int}}/k = 2.5155 + 0.0213i$, which corresponds to $\epsilon^{\text{int}}/\epsilon = 6.3273 + 0.1072i$, $\mu^{\text{int}}/\mu = 1$) were located along the x axis (the center of the first sphere was at the origin of the reference frame and the center of the other had positive x-coordinate) and the scattering plane was at $\varphi = 0$. The size parameter in this case was $ka = 7.86$. The angular dependences of $i_{11} = |S_1|^2$ and $i_{22} = |S_2|^2$ for which data is available are plotted in Fig. 5. In our computations we used $p = 21$ which is the same as the value used in the computations with vector wavefunctions by [30]. The theoretical results using the present method and the method used by Xu and Gustafson are almost on top of each other and so both of them agree well with the experimental data.

The case shown in Fig. 6 presents 15 sphere configuration, where the larger spheres were made of BK7 glass and are the same as in the case shown in Fig. 5. The smaller 12 spheres were acrylic (refractive index $k^{\text{int}}/k = 1.615 + 0.008i$, which corresponds to $\epsilon^{\text{int}}/\epsilon = 2.6082 + 0.0258i$, $\mu^{\text{int}}/\mu = 1$). All neighboring spheres

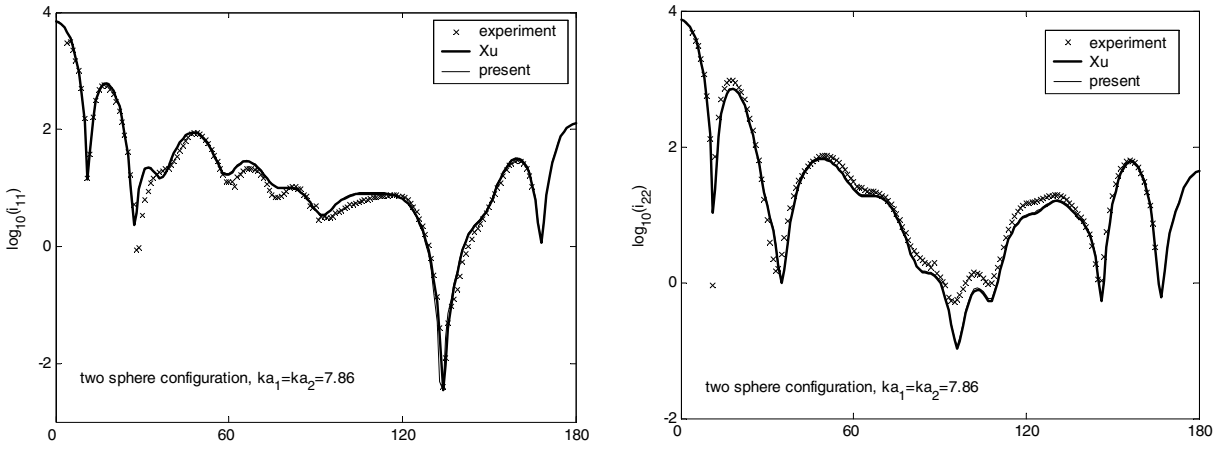

Fig. 5. Comparison of computations using the present theory with theory and experiments of Xu and Gustafson [30] for amplitudes of the scattering matrix entries. The scattering agglomerate consists of two contacting spheres of the same size and dielectric properties.

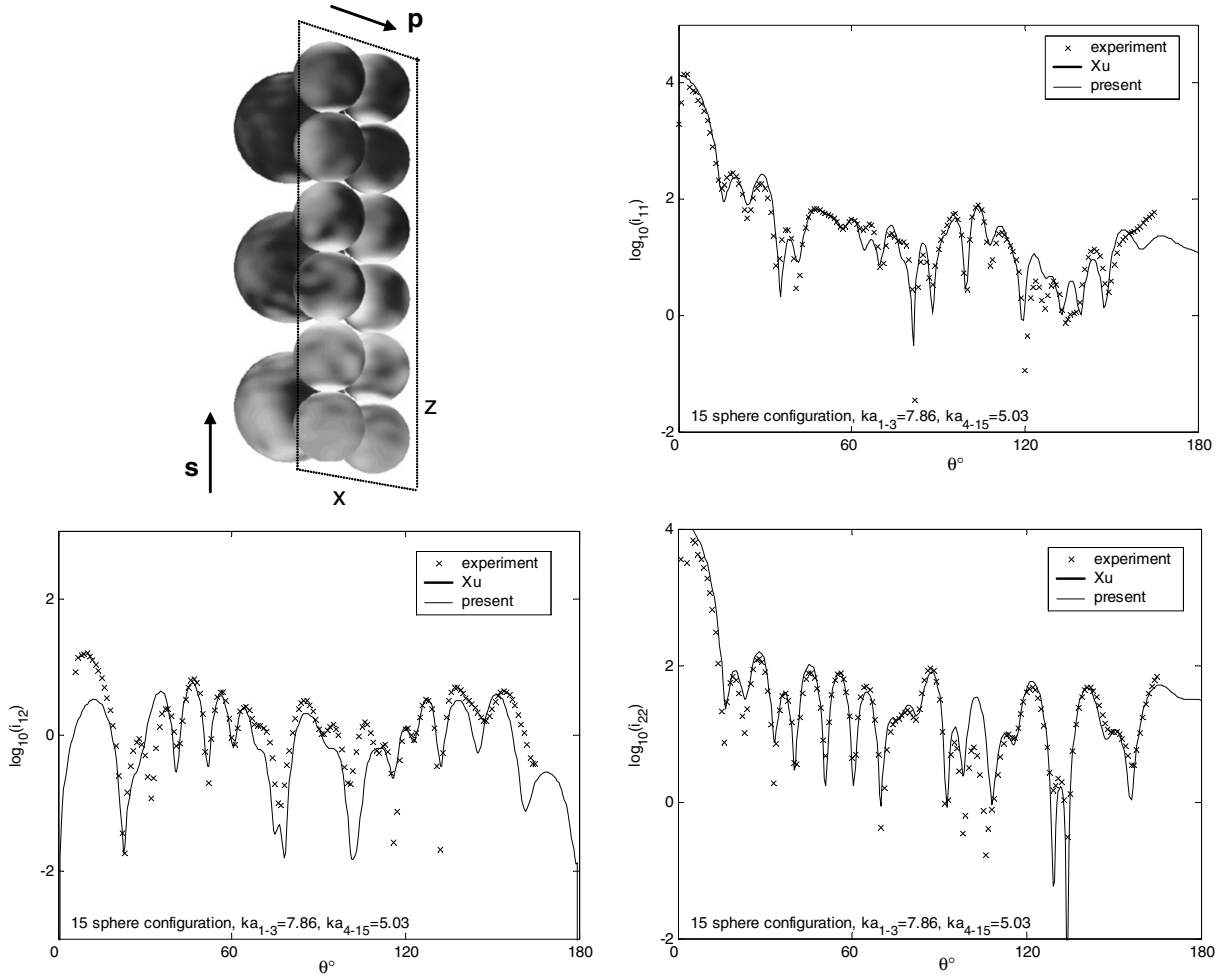

Fig. 6. The same as in Fig. 5, but for 15 sphere agglomerate of spheres of different size and properties (shown in the top right picture). The shades of gray here show distribution of $\log_{10} e$, where e is the energy density over the surface of the scatterers for the x-polarized incident plane wave. Our computational results and those of Ref. [30] are indistinguishable.

were in contact. The aggregate was oriented by such way that the chain of the larger spheres defines the z axis and the centers of the 12 smaller spheres are located in the xz plane. The scattered plane is tilted by angle $\varphi = -3.5°$. In our computations we used a truncation number of $p = 21$. The results of our computations visually coincide with computations of Xu and Gustafson, and also agree well with experiments. Here also the angular dependence of $i_{12} = |S_3|^2$ is provided.

6. Discussion

As soon as the method and relations for translation of multipole solutions has been validated using example multiple scattering problems, its applications can be extended to solution of scattering problems from single or multiple bodies of an arbitrary shape. The method where this can be applied efficiently is the boundary element method enhanced by the fast multipole methods (FMM). As a boundary integral formulation is used in the form of the EFIE (electric field integral equation) or similar (e.g. [7]) and the boundary is discretized the problem reduces to the problem of solution of a large linear system representing sums of singularities on the domain boundary. These sums can be computed in a fast way using the FMM, for which translation operators are in the core of the algorithm. While the method based on the signature functions and translation of its samples using the diagonal forms of the translation operators is in more common use [7,9], for low and

moderate frequency problems methods based on function representation via their multipole and local expansion coefficients with matrix-based translation operators can be comparable or more efficient, as they provide more compact function representation, do not require filtering procedures, and have complexity $O(p^3)$ if using rotation-coaxial translation decomposition. Some results and comparisons for the FMM for the scalar Helmholtz equation can be found in Ref. [14] and the results of use of the BEM/FMM for solution of this equation for large scale problems are reported recently in Ref. [17].

Furthermore, approximate translations of the vector fields, such as the electric field, being performed in a straightforward way require translation of three field components which increases the size of representation three times compared to the scalar case. Moreover this may be a source of additional errors and non-zero divergence of the computed solution as these components are not independent and connected via the divergence free conditions. So as the method of scalar potentials reduces the size of vector field representation and provides solenoidal fields as solutions, we consider it as a promising method for solution of Maxwell equations for complex shaped domains at low and moderate frequencies using the FMM. In this context we showed how the basic singularities (the dyadic Green's function or the Hertzian dipole) can be expressed via the Debye potentials, for which the translation theory developed in the present paper can be applied.

7. Conclusions

We have developed a theory that enables the solution of the Maxwell equations via reduction of these equations to two scalar Helmholtz equations. The translation theory is modified to reduce all operations with vector functions to operations with the scalar potentials. The theory was validated by solution of the scattering problem from several spheres using theoretical and a numerical error check in boundary conditions and comparisons with theoretical and experimental results of other authors. The theory and computational methods based on the method presented can be developed further for the efficient solution of various electromagnetic scattering problems.

Acknowledgment

We thank the reviewers of this paper for their comments. This lead to the derivation of the error bounds for the multiple scattering problem.

Appendix A

A.1. Operator $\mathscr{D}_{\mathbf{r}\times\mathbf{t}}$

The simplest (while not the most elegant) way to obtain representation of operator $\mathscr{D}_{\mathbf{r}\times\mathbf{t}}$ is to use a direct method. In this way we have

$$\begin{aligned}\mathscr{D}_{\mathbf{r}\times\mathbf{t}} &= (\mathbf{r}\times\mathbf{t})\cdot\nabla = (yt_z - zt_y)\frac{\partial}{\partial x} + (zt_x - xt_z)\frac{\partial}{\partial y} + (xt_y - yt_x)\frac{\partial}{\partial z}\\ &= \frac{i}{2}kr\{t_z\sin\theta[\mathrm{e}^{-\mathrm{i}\varphi}\mathscr{D}_{x+\mathrm{i}y} - \mathrm{e}^{\mathrm{i}\varphi}\mathscr{D}_{x-\mathrm{i}y}] + (t_x - \mathrm{i}t_y)[\mathrm{e}^{\mathrm{i}\varphi}\sin\theta\mathscr{D}_z - \cos\theta\mathscr{D}_{x+\mathrm{i}y}]\\ &\quad -(t_x + \mathrm{i}t_y)[\mathrm{e}^{-\mathrm{i}\varphi}\sin\theta\mathscr{D}_z - \cos\theta\mathscr{D}_{x-\mathrm{i}y}]\}.\end{aligned} \tag{131}$$

According to Eqs. (14) and (15) operators $\mathscr{D}_{x\pm\mathrm{i}y}$ and $\mathscr{D}_z$ act on the spherical basis functions $R_n^m(\mathbf{r})$ as follows:

$$\begin{aligned}\mathscr{D}_z[R_n^m(\mathbf{r})] &= a_{n-1}^m R_{n-1}^m(\mathbf{r}) - a_n^m R_{n+1}^m(\mathbf{r}),\\ \mathscr{D}_{x\pm\mathrm{i}y}[R_n^m(\mathbf{r})] &= b_{n+1}^{\mp m-1} R_{n+1}^{m\pm1}(\mathbf{r}) - b_n^{\mp m} R_{n-1}^{m\pm1}(\mathbf{r}),\end{aligned} \tag{132}$$

where coefficients a_n^m and b_n^m are specified by Eqs. (16) and (17). Then we can use properties of spherical harmonics (10) to obtain

$$\mathscr{D}_{\mathbf{r}\times\mathbf{t}}[R_n^m(\mathbf{r})] = -\mathrm{i}mt_z R_n^m(\mathbf{r}) + \frac{i}{2}[(t_x + \mathrm{i}t_y)c_n^{m-1}R_n^{m-1}(\mathbf{r}) + (t_x - \mathrm{i}t_y)c_n^m R_n^{m+1}(\mathbf{r})], \tag{133}$$

where the coefficients c_n^m are specified by Eq. (42). Finally, to get the matrix representation of the operator we note that

$$\begin{aligned}\mathscr{D}_{\mathbf{r}\times\mathbf{t}}\left[\sum_{n=0}^{\infty}\sum_{m=-n}^{n}\chi_n^m R_n^m(\mathbf{r})\right] &= \sum_{n=0}^{\infty}\sum_{m=-n}^{n}\chi_n^m \mathscr{D}_{\mathbf{r}\times\mathbf{t}}[R_n^m(\mathbf{r})]\\ &= \sum_{n=0}^{\infty}\sum_{m=-n}^{n}\chi_n^m\{-\mathrm{i}mt_z R_n^m(\mathbf{r}) + \frac{i}{2}[(t_x+\mathrm{i}t_y)c_n^{m-1}R_n^{m-1}(\mathbf{r}) + (t_x - it_y)c_n^m R_n^{m+1}(\mathbf{r})]\}\\ &= \sum_{n=0}^{\infty}\sum_{m=-n}^{n}\widehat{\chi}_n^m R_n^m(\mathbf{r}) = \sum_{n=0}^{\infty}\sum_{m=-n}^{n}\left[\sum_{n'=0}^{\infty}\sum_{m'=-n'}^{n'}(\mathbf{D}_{\mathbf{r}\times\mathbf{t}})_{nn'}^{mm'}\chi_{n'}^{m'}\right]R_n^m(\mathbf{r}).\end{aligned} \tag{134}$$

This yields Eq. (40).

Another way to derive Eq. (40) is to note that $\mathscr{D}_{\mathbf{r}\times\mathbf{t}}$ is nothing but an infinitesimal rotation operator, which describes rotation by angle $\mathrm{d}\delta$ about axis directed as $\mathbf{t}$. Indeed for such small rotation transform we have

$$\mathbf{r}' = \mathbf{r} + \mathrm{d}\mathbf{r}', \quad \mathrm{d}\mathbf{r}' = (\mathbf{t}\times\mathbf{r})\mathrm{d}\delta, \quad \mathrm{d}\mathbf{r}'\cdot\nabla\psi = (\mathbf{t}\times\mathbf{r})\cdot\nabla\psi\,\mathrm{d}\delta. \tag{135}$$

Using the Taylor expansion, we have

$$\psi(\mathbf{r}+\mathrm{d}\mathbf{r}') = \psi(\mathbf{r}) + \mathrm{d}\mathbf{r}'\cdot\nabla\psi = \psi(\mathbf{r}) + (\mathbf{t}\times\mathbf{r})\cdot\nabla\psi\,\mathrm{d}\delta. \tag{136}$$

On the other hand this is a rotation described by real rotation matrix $\mathbf{Q}(\mathrm{d}\delta)$:

$$\psi(\mathbf{r}+\mathrm{d}\mathbf{r}') = \mathscr{R}ot(\mathbf{Q}(\mathrm{d}\delta))[\psi(\mathbf{r})]. \tag{137}$$

Comparing Eqs. (136) and (137), we can see that

$$\mathscr{D}_{\mathbf{r}\times\mathbf{t}} = -\frac{\mathrm{d}}{\mathrm{d}\delta}\mathscr{R}ot(\mathbf{Q}(\delta))\Big|_{\delta=0}. \tag{138}$$

Now we can use a result for representation of infinitesimal rotation operator in the space of expansion coefficients [14], which results in Eq. (40). Note that this operator became especially simple (diagonal) when the rotation axis is $\mathbf{i}_z$. In this case the small rotation angle δ is related to the spherical polar angle φ alone, and we have

$$\mathscr{D}_{\mathbf{r}\times\mathbf{i}_z}[R_n^m(\mathbf{r})] = -\frac{\mathrm{d}}{\mathrm{d}\delta}\mathscr{R}ot(\mathbf{Q}(\delta))[R_n^m(\mathbf{r})]\Big|_{\delta=0} = -j_n(kr)\frac{\partial}{\partial\varphi}Y_n^m(\theta,\varphi) = -\mathrm{i}mj_n(kr)Y_n^m(\theta,\varphi) = -\mathrm{i}mR_n^m(\mathbf{r}). \tag{139}$$

This results in the conversion operators (46). One also can see that if we set $t_x = t_y = 0$, $t_z = 1$ in Eq. (133), we obtain the same result. In fact, Eq. (133) can be thought of as a result of infinitesimal rotations about the axes x, y, and z, since the infinitesimal rotations commute and so rotation about axis $\mathbf{t}$ can be decomposed into three Cartesian components.

A.2. Operator $\mathscr{D}_{\mathbf{r}\cdot\mathbf{t}}$

First we consider action of operator

$$(\mathbf{r}\cdot\nabla)(\mathbf{t}\cdot\nabla) = kr\frac{\partial}{\partial r}\mathscr{D}_{\mathbf{t}} \tag{140}$$

on the spherical basis functions $R_n^m(\mathbf{r})$, where $\mathscr{D}_{\mathbf{t}}$ is defined by Eq. (14). So we obtain

$$kr\frac{\partial}{\partial r}\mathscr{D}_{\mathbf{t}}[R_n^m] = \frac{k^2 r}{2}\left\{t_{x-\mathrm{i}y}[b_{n+1}^{-m-1}R_{n+1}'^{m+1} - b_n^m R_{n-1}'^{m+1}] + t_{x+\mathrm{i}y}[b_{n+1}^{m-1}R_{n+1}'^{m-1} - b_n^{-m}R_{n-1}'^{m-1}] + 2t_z[a_{n-1}^m R_{n-1}'^m - a_n^m R_{n+1}'^m]\right\}, \tag{141}$$

where

$$R_n'^m(\mathbf{r}) = j_n'(kr)Y_n^m(\theta,\varphi), \quad t_{x\pm\mathrm{i}y} = t_x \pm \mathrm{i}t_y. \tag{142}$$

Further we can express functions $R_n^m(\mathbf{r})$ in the form

$$R_n^m(\mathbf{r}) = \frac{1}{\alpha_n^m} r^{-n} j_n(kr) \underline{R}_n^m(\mathbf{r}), \tag{143}$$

where $\underline{R}_n^m(\mathbf{r})$ are elementary normalized solutions of the Laplace equation in spherical coordinates

$$\underline{R}_n^m(\mathbf{r}) = \alpha_n^m r^n Y_n^m(\theta,\varphi), \quad \alpha_n^m = (-1)^n i^{-|m|} \sqrt{\frac{4\pi}{(2n+1)(n-m)!(n+m)!}}. \tag{144}$$

It was shown recently [16] that these functions satisfy the following relation:

$$\begin{aligned}(\mathbf{r}\cdot\mathbf{t})\underline{R}_n^m = &-\frac{\mathrm{i}t_{x-\mathrm{i}y}(n+m+2)(n+m+1)\underline{R}_{n+1}^{m+1}}{2(2n+1)}\\ &-\frac{\mathrm{i}t_{x+\mathrm{i}y}(n-m+2)(n-m+1)\underline{R}_{n+1}^{m-1}+2t_z(n+m+1)(n-m+1)\underline{R}_{n+1}^m}{2(2n+1)}\\ &+r^2\frac{\mathrm{i}t_{x-\mathrm{i}y}\underline{R}_{n-1}^{m+1}+\mathrm{i}t_{x+\mathrm{i}y}\underline{R}_{n-1}^{m-1}-2t_z\underline{R}_{n-1}^m}{2(2n+1)}.\end{aligned} \tag{145}$$

Therefore, since $\mathscr{D}_{\mathbf{r}\cdot\mathbf{t}} = (\mathbf{r}\cdot\nabla)(\mathbf{t}\cdot\nabla) + k^2(\mathbf{r}\cdot\mathbf{t})$ we can combine the above expressions to determine

$$\begin{aligned}\mathscr{D}_{\mathbf{r}\cdot\mathbf{t}}[R_n^m] = &-\frac{k}{2}\{t_{x+\mathrm{i}y}[b_n^{-m}(n-1)R_{n-1}^{m-1}+(n+2)b_{n+1}^{m-1}R_{n+1}^{m-1}]+t_{x-\mathrm{i}y}[b_n^m(n-1)R_{n-1}^{m+1}+(n+2)b_{n+1}^{-m-1}R_{n+1}^{m+1}]\\ &-2t_z[(n-1)a_{n-1}^m R_{n-1}^m+(n+2)a_n^m R_{n+1}^m]\}.\end{aligned} \tag{146}$$

In this derivation we use definition of spherical basis functions $R_n^m(\mathbf{r})$ via orthonormal harmonics (9), (10), relations (143) and (144), and well-known relations between the spherical Bessel functions of different order and their derivatives [1]. As action of $\mathscr{D}_{\mathbf{r}\cdot\mathbf{t}}$ on basis functions is known, expressions for the matrix representation of this operator, $\mathbf{D}_{\mathbf{r}\cdot\mathbf{t}}$ can be obtained in the same way as we obtained $\mathbf{D}_{\mathbf{r}\times\mathbf{t}}$ (see Eq. (134)). The final result is written out in Eq. (41).

Appendix B

B.1. Error bound for single mode translation

To derive Eq. (113) we use the integral representation of the entries of the translation matrix (see [14]):

$$(S|R)_{nn'}^{mm'}(\mathbf{r}_{q'q}) = \sum_{n''=|n-n'|}^{n+n'}(2n''+1)i^{n''}h_{n''}(kr_{q'q})i^{n-n'}\int_{S_u}P_{n''}\left(\frac{\mathbf{s}\cdot\mathbf{r}_{q'q}}{r_{q'q}}\right)Y_{n'}^{m'}(\mathbf{s})Y_n^{-m}(\mathbf{s})\mathrm{d}S(\mathbf{s}), \tag{147}$$

where integration is taken over the surface of unit sphere, S_u. Substituting this into the definition of $\boldsymbol{\delta}_{n'}^{(q'q)}$, Eq. (112), and using Eq. (111) and the addition theorem for spherical harmonics, we obtain

$$\begin{aligned}\boldsymbol{\delta}_{n'}^{(q'q)} &= \sum_{n=p}^{\infty} j_n(ka_q)\sum_{n''=|n-n'|}^{n+n'}(2n''+1)i^{n''}h_{n''}(kr_{q'q})i^{n-n'}\\ &\quad\times\int_{S_u}P_{n''}\left(\frac{\mathbf{s}\cdot\mathbf{r}_{q'q}}{r_{q'q}}\right)\left(\sum_{m=-n}^{n}Y_n^{-m}(\mathbf{s})Y_n^m(\mathbf{s}')\right)\left(\sum_{m'=-n'}^{n'}\mathbf{E}_{n'}^{(\mathrm{scat},q')m'}Y_{n'}^{m'}(\mathbf{s})\right)\mathrm{d}S(\mathbf{s})\\ &= \sum_{n=p}^{\infty}(2n+1)j_n(ka_q)\sum_{n''=|n-n'|}^{n+n'}(2n''+1)i^{n''}h_{n''}(kr_{q'q})i^{n-n'}\frac{1}{4\pi}\int_{S_u}P_{n''}\left(\frac{\mathbf{s}\cdot\mathbf{r}_{q'q}}{r_{q'q}}\right)P_n(\mathbf{s}\cdot\mathbf{s}')\mathbf{E}_{n'}^{(q')}(\mathbf{s})\mathrm{d}S(\mathbf{s}).\end{aligned} \tag{148}$$

Note then that for arbitrary unit vectors $|\mathbf{s}''| = |\mathbf{s}'| = 1$ we have using the Cauchy–Schwarz inequality and the norm of the Legendre polynomials

$$\frac{1}{4\pi}\int_{S_u}|P_{n''}(\mathbf{s}\cdot\mathbf{s}'')||P_n(\mathbf{s}\cdot\mathbf{s}')|\mathrm{d}S(\mathbf{s}) \leqslant \left(\frac{1}{4\pi}\int_{S_u}|P_{n''}(\mathbf{s}\cdot\mathbf{s}'')|^2\mathrm{d}S(\mathbf{s})\right)^{1/2}\left(\frac{1}{4\pi}\int_{S_u}|P_{n''}(\mathbf{s}\cdot\mathbf{s}'')|^2\mathrm{d}S(\mathbf{s})\right)^{1/2}$$
$$= \left(\frac{1}{2}\int_{-1}^{1}P_{n''}^2(\mu)\mathrm{d}\mu\right)^{1/2}\left(\frac{1}{2}\int_{-1}^{1}P_n^2(\mu)\mathrm{d}\mu\right)^{1/2} = \frac{1}{(2n+1)^{1/2}(2n''+1)^{1/2}}. \quad (149)$$

This bounds functions (148) as follows:

$$|\boldsymbol{\delta}_{n'}^{(q'q)}| \leqslant \sum_{n=p}^{\infty}(2n+1)|j_n(ka_q)|\sum_{n''=|n-n'|}^{n+n'}(2n''+1)|h_{n''}(kr_{q'q})|\frac{1}{4\pi}\int_{S_u}\left|P_{n''}\left(\frac{\mathbf{s}\cdot\mathbf{r}_{q'q}}{r_{q'q}}\right)\right||P_n(\mathbf{s}\cdot\mathbf{s}')||\mathbf{E}_{n'}^{(q')}(\mathbf{s})|\mathrm{d}S(\mathbf{s})$$
$$\leqslant \max_{\mathbf{s}}|\mathbf{E}_{n'}^{(q')}(\mathbf{s})|\sum_{n=p}^{\infty}(2n+1)^{1/2}|j_n(ka_q)|\sum_{n''=|n-n'|}^{n+n'}(2n''+1)^{1/2}|h_{n''}(kr_{q'q})|. \quad (150)$$

Note that $|h_{n''}|$ is a monotonically growing function of n'' (e.g. [14]). This means that

$$\sum_{n''=|n-n'|}^{n+n'}(2n''+1)^{1/2}|h_{n''}(kr_{q'q})| \leqslant |h_{n+n'}(kr_{q'q})|\sum_{n''=|n-n'|}^{n+n'}(2n''+1)^{1/2} \leqslant (2n+1)^{1/2}(2n'+1)|h_{n+n'}(kr_{q'q})|. \quad (151)$$

The latter bound follows from the fact $n' < p \leqslant n$ and Cauchy's inequality. Substituting Eq. (151) into Eq. (150), we obtain

$$|\boldsymbol{\delta}_{n'}^{(q'q)}| \leqslant (2n'+1)\max_{\mathbf{s}}|\mathbf{E}_{n'}^{(q')}(\mathbf{s})|\sum_{n=p}^{\infty}(2n+1)|j_n(ka_q)||h_{n+n'}(kr_{q'q})|. \quad (152)$$

Further we use the corollary of a theorem proven in Ref. [14] (p. 451):

$$|h_{n+n'}(kb+ka)| < \alpha_{n'}|h_n(kb)|,$$
$$\alpha_{n'} = \begin{cases} 1, & n' \leqslant ka, \\ \left(\frac{e\pi}{2n'-1}\right)^{1/2}|j_{n'}(ka)|^{-1}, & n' > ka \end{cases} \qquad ka, kb > 0, \quad n = 0, 1, \ldots, \quad (153)$$

where the inequality for $n' \leqslant ka$ follows from the prove. This results in Eq. (113).

B.2. Estimate of the Gegenbauer series residual

Consider the behavior of the function

$$\epsilon_n = (2n+1)|j_n(ka)||h_n(kb)|, \quad b > a, \quad n \gg 1, \quad n+\frac{1}{2} > ka. \quad (154)$$

In this case the following asymptotics apply to the absolute values of spherical Bessel and Hankel functions [1]:

$$|j_n(ka)| = \left(\frac{\pi}{2ka}\right)^{1/2}|J_{n+1/2}(ka)| \sim \left(\frac{\pi}{2ka}\right)^{1/2}2^{1/3}\left(n+\frac{1}{2}\right)^{-1/3}|\mathrm{Ai}(2^{1/3}\eta_n^{(a)})|,$$
$$|h_n(kb)| \sim \left(\frac{\pi}{2kb}\right)^{1/2}|Y_{n+1/2}(kb)| \sim \left(\frac{\pi}{2kb}\right)^{1/2}2^{1/3}\left(n+\frac{1}{2}\right)^{-1/3}|\mathrm{Bi}(2^{1/3}\eta_n^{(b)})|, \quad (155)$$
$$\eta_n^{(a)} = \frac{n-ka+1/2}{(ka)^{1/3}}, \quad \eta_n^{(b)} = \frac{n-kb+1/2}{(kb)^{1/3}},$$

where Ai and Bi the Airy functions of the first and second kind [1].

The following two lemmas provide bounds for these functions for positive arguments.

Lemma 1. *For $x > 0$ the Airy function of the first kind* $\mathrm{Ai}(x)$ *is bounded by*

$$\mathrm{Ai}(x) < Af(x), \quad f(x) = \exp\left(-\frac{2}{3}x^{3/2}\right), \quad A = \mathrm{Ai}(0) = 3^{-2/3}/\Gamma(2/3) < 0.3351. \quad (156)$$

Proof. Consider the function $R(x) = \mathrm{Ai}(x)/f(x) > 0$. Since $\mathrm{Ai}(x)$ satisfies $\mathrm{Ai}''(x) = x\mathrm{Ai}(x)$ and $f'(x) = -x^{1/2}f(x)$, $f''(x) = (x - \frac{1}{2}x^{-1/2})f(x)$ we can determine that $R''(x) = 2x^{1/2}R'(x) + \frac{1}{2}x^{-1/2}R(x)$. Assume then that there exists $x = x_*$ for which $R'(x_*) = 0$. For this point $R''(x_*) = \frac{1}{2}x_*^{-1/2}R(x_*) > 0$ so any extremum of $R(x)$ should be a minimum and, therefore, the minimum if exists is unique. We have then

$$\forall x > 0, \quad \frac{R(x)}{R(x_*)} = \frac{\mathrm{Ai}(x)}{R(x_*)f(x)} \geqslant 1, \tag{157}$$

which contradicts to the asymptotic behavior of $\mathrm{Ai}(x)$ at large x [1]:

$$\frac{\mathrm{Ai}(x)}{R(x_*)f(x)} \sim \frac{1}{R(x_*)x^{1/4}} \to 0. \tag{158}$$

Thus, there is no minima of $R(x)$ for finite x, and $R(x)$ decays monotonically, since $R'(0) = \mathrm{Ai}'(0)/f(0) < 0$. This means that $f(x) > \mathrm{Ai}(x)/\mathrm{Ai}(0)$. □

Lemma 2. *For $x > 0$ the Airy function of the second kind $Bi(x)$ is bounded by*

$$Bi(x) < Bg(x), \quad g(x) = \exp\left(\frac{2}{3}x^{3/2}\right), \quad Bi(0) < B < 0.6776 < 1.102Bi(0). \tag{159}$$

Proof. Consider function $G(x) = Bg(x) - \mathrm{Bi}(x)$ for some positive constant B, assuming that $G(x) > 0$. Since $\mathrm{Bi}(x)$ satisfies $\mathrm{Bi}''(x) = x\mathrm{Bi}(x)$ and $g'(x) = x^{1/2}g(x)$, $g''(x) = (x + \frac{1}{2}x^{-1/2})g(x)$ we can determine that $G''(x) = B\frac{1}{2}x^{-1/2}g(x) + xG(x) > 0$. This means that $G'(x)$ grows monotonically. Since $G'(0) = -\mathrm{Bi}'(0) < 0$ while $G(x) \to \infty$ as $x \to \infty$ (at large x, $\mathrm{Bi}(x)/g(x) = \mathrm{O}(x^{-1/4})$ [1]) this function has a single zero at some $x = x_*$, which is the minimum of $G(x)$ as $G''(x_*) > 0$. Note that x_* depends on B, while it is more convenient to use the inverse function $B(x_*)$ since $G'(x_*) = 0$ provides

$$B = \frac{\mathrm{Bi}'(x_*)}{x_*^{1/2}g(x_*)}. \tag{160}$$

To guarantee that $G(x) > 0$ for any $x > 0$ we request that $G(x_*) > 0$ which is equivalent to $B > \mathrm{Bi}(x_*)/g(x_*)$ and provides a constraint for selection of point x_*:

$$\frac{x_*^{1/2}\mathrm{Bi}(x_*)}{\mathrm{Bi}'(x_*)} \leqslant 1, \tag{161}$$

which otherwise can be selected arbitrarily. Choosing $x_* = 0.4$ we obtain (one can use tables for $\mathrm{Bi}(x)$ and $\mathrm{Bi}'(x)$ [1])

$$\frac{x_*^{1/2}\mathrm{Bi}(x_*)}{\mathrm{Bi}'(x_*)} \approx 0.9996 < 1, \quad B = \frac{\mathrm{Bi}'(x_*)}{x_*^{1/2}g(x_*)} \approx 0.677599895 < 0.6776. \tag{162}$$

Note then that $B > \mathrm{Bi}(0) = 3^{1/2}\mathrm{Ai}(0) \approx 0.6149$ since $\mathrm{Bi}(0)g(0.4) - \mathrm{Bi}(0.4) < 0$. □

We note that for non-positive x we have $|\mathrm{Bi}(x)| \leqslant \mathrm{Bi}(0) < B$. Therefore, if we redefine $\eta_n^{(b)}$ as

$$\eta_n^{(b)} = \begin{cases} (kb)^{-1/3}(n - kb + 1/2), & n > kb - 1/2, \\ 0, & n \leqslant kb - 1/2, \end{cases} \tag{163}$$

we obtain from (154), (155), (156), and (159) an estimate valid for any $n + \frac{1}{2} > ka$, $n \gg 1$

$$\epsilon_n \lesssim 1.2\frac{(n+1/2)^{1/3}}{\delta^{1/2}ka}\exp\left\{-\frac{1}{3}((2\eta_n^{(a)})^{3/2} - (2\eta_n^{(b)})^{3/2})\right\} \sim \frac{n^{1/3}}{\delta^{1/2}ka}\exp\left\{-\frac{1}{3}((2\eta_n^{(a)})^{3/2} - (2\eta_n^{(b)})^{3/2})\right\}. \tag{164}$$

Note that due to exponential decay of these functions with respect to n the first term in the series for ϵ_p^s provides estimate of the entire sum:

$$\epsilon_p^s = \sum_{n=p}^{\infty} \epsilon_n = \epsilon_p + \mathrm{O}(\epsilon_{p+1}) \sim \epsilon_p. \tag{165}$$

References

[1] M. Abramowitz, I.A. Stegun (Eds.), Handbook of Mathematical Functions, National Bureau of Standards, Washington, DC, 1964.
[2] C.F. Bohren, D.R. Huffman, Absorption and Scattering of Light by Small Particles, Wiley, New-York, 1983.
[3] J.J. Bowman, T.B.A. Senior, P.L.E. Uslenghi, Electromagnetic and Acoustic Scattering by Simple Shapes, Hemisphere, New York, 1987.
[4] J.H. Brunning, Y.T. Lo, Multiple scattering of EM waves by spheres, parts I and II, IEEE Trans. Antennas Propag. AP-19 (3) (1971) 378–400.
[5] W.C. Chew, Recurrence relations for three-dimensional scalar addition theorem, J. Electromagnet. Waves Appl. 6 (2) (1992) 133–142.
[6] W.C. Chew, Y.M. Wang, Efficient ways to compute the vector addition theorem, J. Electromagnet. Waves Appl. 7 (5) (1993) 651–665.
[7] W.C. Chew, J.-M. Jin, E. Michielssen, J. Song, Fast and Efficient Algorithms in Computational Electromagnetics, Artech House, Boston, 2001.
[8] O.R. Cruzan, Translational addition theorems for spherical vector wave functions, Q. Appl. Math. 20 (1962) 33–39.
[9] E. Darve, The fast multipole method I: Error analysis and asymptotic complexity, SIAM J. Numer. Anal. 38 (1) (2000) 98–128.
[10] P. Debye, Der Lichtdruck auf Kugeln von beliebigem Material, Annal. Phys. (Leipzig) 30 (1909) 57–136.
[11] M.A. Epton, B. Dembart, Multipole translation theory for the three-dimensional Laplace and Helmholtz equations, SIAM J. Sci. Comput. 16 (1995) 865–897.
[12] N.A. Gumerov, R. Duraiswami, Computation of scattering from N spheres using multipole reexpansion, J. Acoust. Soc. Am. 112 (6) (2002) 2688–2701.
[13] N.A. Gumerov, R. Duraiswami, Recursions for the computation of multipole translation and rotation coefficients for the 3-D Helmholtz equation, SIAM J. Sci. Comput. 25 (4) (2003) 1344–1381.
[14] N.A. Gumerov, R. Duraiswami, Fast Multipole Methods for the Helmholtz Equation in Three Dimensions, Elsevier, Oxford, 2004.
[15] N.A. Gumerov, R. Duraiswami, Computation of scattering from clusters of spheres using the fast multipole method, J. Acoust. Soc. Am. 117 (4) (2005) 1744–1761, Part 1.
[16] N.A. Gumerov, R. Duraiswami, Fast multipole method for the biharmonic equation in three dimensions, J. Comput. Phys. 215 (1) (2006) 363–383.
[17] N.A. Gumerov, R. Duraiswami, FMM accelerated BEM for 3D Laplace and Helmholtz equationsProceedings of the International Conference on Boundary Element Techniques VII, BETEQ-7, Paris, France, EC Ltd., UK, 2006, pp. 79–84.
[18] J.D. Jackson, Classical Electrodynamics, Wiley, New York, 1998.
[19] S. Koc, W.C. Chew, Calculation of acoustical scattering from a cluster of scatterers, J. Acoust. Soc. Am. 103 (2) (1998) 721–734.
[20] D.W. Mackowski, Analysis of radiative scattering for multiple sphere configurations, Proc. R. Soc. London Ser. A 433 (1991) 599–614.
[21] M.I. Mishchenko, L.D. Travis, D.W. Mackowski, T-matrix computations of light scattering by nonspherical particles: a review, J. Quant. Spectrosc. Radiat. Transfer 55 (1996) 535–575.
[22] V. Rokhlin, Diagonal forms of translation operators for the Helmholtz equation in three dimensions, Appl. Comp. Harmonic Anal. 1 (1993) 82–93.
[23] S. Stein, Addition theorems for spherical wave functions, Q. Appl. Math. 19 (1961) 15–24.
[24] V.K. Varadan, V.V. Varadan, Acoustic, Electromagnetic and Elastic Wave Scattering: Focus on the T-Matrix Approach, Pergamon, New York, 1980.
[25] Y.M. Wang, W.C. Chew, A recursive T-matrix approach for the solution of electromagnetic scattering by many spheres, IEEE Trans. Antennas Propagat. 41 (12) (1993) 1633–1639.
[26] P.C. Waterman, R. Truell, Multiple scattering of waves, J. Math. Phys. 2 (1961) 512–537.
[27] Y.-L. Xu, Calculation of the addition coefficients in electromagnetic multisphere-scattering theory, J. Comput. Phys. 127 (1996) 285–298 (Erratum, J. Comput. Phys. 134 (1997) 200).
[28] Y.-L. Xu, R.T. Wang, Electromagnetic scattering by an aggregate of spheres: theoretical and experimental study of the amplitude scattering matrix, Phys. Rev. E 58 (3) (1998) 3931–3948.
[29] Y.-L. Xu, B.Å.S. Gustafson, Experimental and theoretical results of light scattering by aggregates of spheres, Appl. Opt. 36 (30) (1997) 8026–8030.
[30] Y.-L. Xu, B.Å.S. Gustafson, An analytical solution to electromagnetic multisphere-scattering – the scattering formulation used in codes gmm01f.f and gmm01s.f. <http://www.astro.ufl.edu/~xu/codes/gmm01f/description.pdf>.
[31] G. Mie, Beiträge zur Optik trüber Medien, speziell kolloidaler Metallösungen, Annal. Phys. (Leipzig) 25 (1908) 377–445.